Downloaded from genome.cshlp.org on November 14, 2026 . Published by Cold Spring Harbor Laboratory Press



Genome-wide parent-of-origin DNA methylation analysis reveals the intricacies of the human imprintome and suggests a germline methylation independent establishment of imprinting

Franck Court, Chiharu Tayama, Valeria Romanelli, et al.

Genome Res. published online January 8, 2014
Access the most recent version at doi:10.1101/gr.164913.113

P<P Published online January 8, 2014 in advance of the print journal.

Accepted Manuscript Peer-reviewed and accepted for publication but not copyedited or typeset; accepted manuscript is likely to differ from the final, published version.

Creative Commons License This article is distributed exclusively by Cold Spring Harbor Laboratory Press for the first six months after the full-issue publication date (see http://genome.cshlp.org/site/misc/terms.xhtml). After six months, it is available under a Creative Commons License (Attribution-NonCommercial 3.0 Unported), as described at http://creativecommons.org/licenses/by-nc/3.0/.

Email Alerting Service Receive free email alerts when new articles cite this article - sign up in the box at the top right corner of the article or **click here.**



To subscribe to *Genome Research* go to:
https://genome.cshlp.org/subscriptions

Published by Cold Spring Harbor Laboratory Press

Downloaded from genome.cshlp.org on November 14, 2026 . Published by Cold Spring Harbor Laboratory Press

Genome-wide parent-of-origin DNA methylation analysis reveals the intricacies of human imprinting and suggests a germline methylation independent mechanism of establishment

Franck Court[1,15], Chiharu Tayama[2,15], Valeria Romanelli[1,15], Alex Martin-Trujillo[1,15], Isabel Iglesias-Platas[3], Kohji Okamura[4], Naoko Sugahara[2], Carlos Simón[5], Harry Moore[6], Julie V Harness[7], Hans Keirstead[7], Jose Vicente Sanchez-Mut[8], Elsuke Kaneki[9], Pablo Lapunzina[10], Hidenobu Soejima[11], Norio Wake[9], Manel Esteller [8,12,13], Tsutomu Ogata[14], Kenichiro Hata[2], Kazuhiko Nakabayashi[2,16], David Monk[1,16].

[15] These authors contributed equally to this work.
[16] These authors jointly directed this work.
[#]Correspondence should be addressed to K.N. (nakabaya-k@ncchd.go.jp) or D.M. (dmonk@idibell.cat).

David Monk
Cancer Epigenetics and Biology Program (PEBC)
Bellvitge Biomedical Research Institute (IDIBELL)
Av. Gran Via de L'Hospotalet 199-203
08907 L'Hospitalet de Llobregat, Barcelona,
Spain.

Tel: 0034 93 260 7128
FAX: 0034 2607219

1. Imprinting and Cancer group, Cancer Epigenetic and Biology Program, Institut d'Investigació Biomedica de Bellvitge, Hospital Duran i Reynals, Barcelona, Spain.
2. Department of Maternal-Fetal Biology and Department of Molecular Endocrinology, National Research Institute for Child Health and Development, Tokyo 157-8535, Japan.
3. Servicio de Neonatología, Hospital Sant Joan de Déu, Fundació Sant Joan de Déu, Barcelona, Spain.
4. Department of Systems Biomedicine, National Research Institute for Child Health and Development, 2-10-1 Okura, Setagaya, Tokyo, 157-8535, Japan.
5. Fundación IVI-Instituto Universitario IVI-Universidad de Valencia, INCLIVA, Valencia, Spain.
6. Centre for Stem Cell Biology, Department of Biomedical Science, University of Sheffield, Alfred Denny Building, Sheffield, UK.
7. Reeve-Irvine Research Centre, Sue and Bill Gross Stem Cell Research Center, Department of Anatomy and Neurobiology, School of Medicine, University of California at Irvine, Irvine, CA 92697, USA.
8. Cancer Epigenetics group, Cancer Epigenetic and Biology Program, Institut d'Investigació Biomedica de Bellvitge, Hospital Duran i Reynals, Barcelona, Spain.
9. Department of Obstetrics and Gynecology, Graduate School of Medical Science, Kyushu University, 3-1-1 Maidashi, Higashi-ku, Fukuoka, 812-8582, Japan.

Downloaded from genome.cshlp.org on November 14, 2026 . Published by Cold Spring Harbor Laboratory Press

10. Instituto de Genética Médica y Molecular, CIBERER, IDIPAZ-Hospital Universitario La Paz, Universidad Autónoma de Madrid, Spain.
11. Division of Molecular Genetics and Epigenetics, Department of Biomolecular Sciences, Faculty of Medicine, Saga University, 5-1-1 Nabeshima, Saga, 849-8501, Japan.
12. Department of Physiological Sciences II, School of Medicine, University of Barcelona, Barcelona, Catalonia, Spain.
13. Institucio Catalana de Recerca i Estudis Avançats (ICREA), Barcelona, Catalonia, Spain.
14. Department of Pediatrics, Hamamatsu University School of Medicine, 1-20-1 Handayama, Higashi-ku, Hamamatsu, 431-3192, Japan.

Running title: Screening for human imprinted DMRs.
Key words: Imprinting, DNA methylation, histone modifications, placenta.

Downloaded from genome.cshlp.org on November 14, 2026 . Published by Cold Spring Harbor Laboratory Press

Abstract

Differential methylation between the two alleles of a gene has been observed at imprinted regions, where the methylation of one allele occurs on a parent-of-origin basis, the inactive X-chromosome in females, and at those loci whose methylation is driven by genetic variants. We have extensively characterized imprinted methylation in a substantial range of normal human tissues, reciprocal genome-wide uniparental disomies and hydatidiform moles, using a combination of whole genome bisulphite sequencing and high-density methylation microarrays. This approach allowed us to define methylation profiles at known imprinted domains at base-pair resolution, as well as identifying 21 novel loci harbouring parent-of-origin methylation, 15 of which are restricted to the placenta. We observe that the extent of imprinted differentially methylated regions (DMRs) is extremely similar between tissues, with the exception of the placenta. This extra-embryonic tissue often adopts a different methylation profile compared to somatic tissues. Further we profiled all imprinted DMRs in sperm and embryonic stem cells derived from parthenogenetically-activated oocytes, individual blastomeres and blastocysts to identifying primary DMRs and reveal the extent of reprograming during pre-implantation development. Intriguingly, we find that in contrast to ubiquitous imprints, the majority of placenta-specific imprinted DMRs are unmethylated in sperm and all human embryonic stem cells. Therefore, placental-specific imprinting provides evidence for an inheritable epigenetic state that is independent of DNA methylation and the existence of a novel imprinting mechanism at these loci.

Downloaded from genome.cshlp.org on November 14, 2026 . Published by Cold Spring Harbor Laboratory Press

Introduction

Genomic imprinting is a form of epigenetic regulation that results in expression of either the maternally or paternally inherited allele of a subset of genes (Ramowitz et al. 2011). This imprinted expression of transcripts is crucial for normal mammalian development. In humans loss-of-imprinting of specific loci results in a number of diseases exemplified by the reciprocal growth phenotypes of the Beckwith Wiedemann and Silver Russell syndromes, and the behavioural disorders Angelman and Prader-Willi syndromes (Choufani et al. 2010; Eggermann 2010; Buiting 2010; Mackay & Temple 2010; Kelsey 2010; Kagami et al. 2008). In addition, aberrant imprinting also contributes to multigenic disorders associated with various complex traits and cancer (Kong et al. 2009; Monk et al. 2010).

Imprinted loci contain differentially methylated regions (DMRs) where cytosine methylation marks one of the parental alleles, providing *cis*-acting regulatory elements that influence the allelic expression of surrounding genes. Some DMRs acquire their allelic methylation during gametogenesis, when the two parental genomes are separated, resulting from the cooperation of the *de novo* methyltransferase DNMT3A and its co-factor DNMT3L (Bourc'his et al. 2001; Hata et al. 2002). These primary, or germline, imprinted DMRs are stably maintained throughout somatic development, surviving the epigenetic reprogramming at the oocyte-to-embryo transition (Smallwood et al. 2011; Smith et al. 2012). To confirm that an imprinted DMR functions as an imprinting control region (ICR), disruption of imprinted expression upon genetic deletion of that DMR, either through experimental targeting in mouse or that occurring spontaneously in humans, is required. A subset of DMRs, known as secondary DMRs, acquire methylation during development and are regulated by nearby germline DMRs in a hierarchical fashion (Lopes et al. 2003; Coombes et al. 2003; Kagami et al. 2010).

With the advent of large-scale, base-resolution methylation technologies it is now possible to discriminate allelic methylation dictated by sequence variants from imprinted methylation. Yet, our knowledge of the total number of imprinted DMRs in humans, and their developmental dynamics, remains incomplete, hampered by genetic heterogeneity of human samples.

Here, we present high resolution mapping of human imprinted methylation. We performed whole genome-wide bisulphite sequencing (WGBS) on leukocyte-, brain-, liver- and placenta-derived DNA samples to identify partially methylated regions common to all tissues consistent with imprinted DMRs. We subsequently confirmed the partial methylated states in tissues using high-density methylation microarrays. The parental origin of methylation was determined by comparing microarray data for DNA samples from reciprocal genome-wide uniparental disomy (UPD) samples, in which all chromosomes are inherited from one parent (Lapunzina & Monk 2011), and androgenetic hydatidiform moles, which are created by the fertilization of an oocyte lacking a nucleus by a sperm that endoreduplicates. The use of uniparental disomies and hydatidiform moles meant that our analyses were not subjected to genotype influences, enabling us to characterise all known imprinted DMRs at base-pair resolution, and to identify 21 imprinted domains, which we show are absent in mice. Lastly, we extended our analyses to determine the methylation profiles of all imprinted DMRs in sperm, stem cells derived from parthenogenetically activated metaphase-2 oocyte blastocytes (phES) (Mai et al. 2007; Harness et al. 2011), and stem cells (hES) generated from both six-cell blastomeres and the inner

Downloaded from genome.cshlp.org on November 14, 2026 . Published by Cold Spring Harbor Laboratory Press

cell mass of blastocysts, delineating the extent of embryonic reprogramming that occurs at these loci during human development.

Results

Characterization of parent-of-origin methylation profiles in human tissues using high-resolution approaches

We combined whole-genome bisulphite sequencing (WGBS) with Illumina Infinium HumanMethylation 450K BeadChip arrays to generate methylation profiles. To validate this approach we compared the DNA methylation profiles generated by each method. Methylation scores produced by the two methods are very similar when the same DNA samples were assessed by both techniques (linear regression WGBS vs. Infinium array: leukocytes R^2= 0.92; brain R^2= 0.91; placenta R^2=0.92) (Supplemental Fig. S1). To determine the similarity between normal biparental leukocytes and those from reciprocal genome-wide UPDs we compared the methylation values obtained from the Infinium array. This revealed high correlations between samples indicating that the DNAs were similar, differing only at imprinted loci (linear regression: leukocytes vs. leukocytes R^2=0.95-0.98; mean control leukocytes vs. mean pUPD R^2= 0.98; mean control leukocytes vs. mUPD R^2=0.98; mUPD vs. mean pUPD R^2= 0.97. F-statistics $p<0.001$).

Before we attempted to discover novel imprinted DMRs in the human genome, we wished to determine the effectiveness of the Infinium array to identify known imprinted DMRs. Loci were identified which contained at least three Infinium probes with an averaged minimal difference of 0.3 β-values (absolute methylation difference >30%) between reciprocal genome-wide UPD leukocyte samples, with a prerequisite that the β-values for normal leukocytes should be between these extremes. Using these criteria we identified 818 windows that could be merged into 145 regions harbouring 576 probes incorporating 30 known DMRs within 25 imprinted domains (Table 1; Fig. 1A) (Limma linear model $p<0.05$) and presented with an intermediate methylation profile in all somatic tissues (Fig. 1B). The only imprinted DMRs not found using this approach were the IG-DMR located between *MEG3* and *DLK1* on chromosome 14 as this region does not have probes on this array platform and *IGF2*-DMR0 that only contains a single probe.

Identification of new DMRs within known imprinted domains

In addition to the known imprinted DMRs the Infinium array screen of reciprocal UPDs and tissues samples uncovered several previously unidentified DMRs located within existing imprinted domains. We discovered four maternally methylated CpG islands located between the *SNRPN* and *NDN* genes on chromosome 15, a region associated with the Angelman and Prader-Willi syndromes. The methylation profiles at the *SNRPN*, *NDN* and *MAGEL2* promoters are well established (El-Maarri et al. 2001; Sharp et al. 2010). However, little is known about the intervening ~1 Mb gene-poor region, which is likely to have arisen from an ancient duplication event, since these novel DMRs share 97.8% sequence identity with additional CpG-rich regions in the interval. We confirm the maternal methylation at these four regions using bisulphite PCR and sequencing incorporating heterozygous SNPs in brain and leukocyte DNA (Supplemental Fig. S2A). Further analysis of this region revealed that the promoter region for *MKRN3* and *MIR4508* are also differentially methylated.

Extending our analysis to imprinted domains on other autosomes, we identified an ~600 bp interval of maternal methylation 4 kb 3' to the *ZNF597* gene (Fig.1C). Although the promoter of *ZNF597* is a paternally methylated bidirectional

Downloaded from genome.cshlp.org on November 14, 2026 . Published by Cold Spring Harbor Laboratory Press

silencer presumably responsible for regulating the imprinted expression of both *ZNF597* and *NAA60* (previously known as *NAT15*), this region is unlikely to be the ICR for the domain as its methylation is somatically acquired (Nakabayashi et al. 2011). In addition, WGBS and Infinium array datasets revealed a maternally methylated DMR within intron 2 of *MEG8* within the chromosome 14 imprinted domain (Supplemental Fig. S2B). Lastly, we identify two maternally methylated regions. The first is a ~1 kb CpG island overlapping the promoter of isoform 3 of the *ZNF331* gene, and the second coincides with exon 2 of *DIRAS3* (Supplemental Fig. S2C).

Genome-wide methylation profiling identifies novel imprinted domains

To determine if there are additional imprinted DMRs in the human genome we screened for regions of intermediate methylation common to lymphocyte, brain and liver WGBS datasets. Using a sliding window approach that takes into account 25 consecutive CpG sites and following removal of class 1 transposable elements (LINEs, Alu/SINEs and LTR elements) and satellite DNA, we identified 356 non-overlapping, single copy regions in pair-wise comparisons of tissues, of which 63 loci were common to the all tissues ($0.25 < \text{mean} \pm 1.5\ SD < 0.75$) (Fig. 2A; Supplemental Table S1).

A screen for 3 consecutive partially methylated probes in leukocyte, brain, liver, kidney and muscle Infinium datasets, with a profile consistent with parent-of-origin methylation in the reciprocal UPD leukocyte samples, identified 116 regions (Supplemental Table S1). By combining the 356 regions detected by WGBS and the 116 loci identified by the Infinium array, we identified 64 regions in common which included all known imprinted DMRs and 17 CpG-rich sequences possessing a methylation profiles consistent with imprinting. Using standard bisulphite PCR, we assessed all regions and verified that six regions (*PPIEL*, *WDR27*, *HTR5A*, *WRB*, *NHP2L1*, *ERLIN2* loci) are maternally methylated. The DMR we identify within intron 7 of *ERLIN2* appears to be a retro-insertion of the *CXorf56* pseudogene (also known as *LOC728024*) (Fig. 2B, C; Supplemental Fig. S3; Supplemental Table S1).

To confirm that parent-of-origin transcription occurs near these novel imprinted DMRs, we performed allelic RT-PCR in a panel of tissues with primers that discriminate major variant transcripts within each region. This revealed that the DMRs associated with *WDR27*, *NHP2L1* and *CXorf56* pseudogene regulate allelic expression in an isoform-specific fashion (Fig. 2B, C; Supplemental Fig. S3; Supplemental Table S1). We detect monoallelic expression of a short alternatively polyadenylated *ERLIN2* transcript which independently substantiates the observation that the generation of retrogenes, primarily from the X chromosome, is a common mechanism for generating imprinted loci (Wood et al. 2008; Kanber et al. 2009). Unfortunately, due to the lack of informative polymorphism or expression in available heterozygous tissues, we could not perform allelic expression analysis for *PPIEL*, *HTR5A* and *WRB*.

Histone methylation of H3K4 and DNA methylation are enriched on opposing alleles at imprinted DMRs

GC-rich sequences often coincide with enrichment of H3K4me3, which may act to protect them from *de novo* methylation (Thomson et al. 2010). The H3K4 demethylase KDM1B (also known as AOF1) is required for appropriate establishment of maternal germline methylation for a subset of imprinted DMRs in mouse, suggesting that the presence of H3K4 methylation is refractory to DNA methylation

Downloaded from genome.cshlp.org on November 14, 2026 . Published by Cold Spring Harbor Laboratory Press

deposition in the female germline (Ciccone et al. 2009). By comparing publically available datasets for ChIP-seq for H3K4me3 and methylated DNA immunoprecipitation (meDIP-seq) from blood and brain, we observe co-enrichment of these opposing epigenetic marks at 89.5% of imprinted DMRs, consistent with differential active and repressive chromatin states on homologous chromosomes. For a limited number of informative regions we were able to confirm H3K4me3 precipitation on the unmethylated allele (Fig. 3C). In most cases the methylation profile of maternally methylated DMRs is more closely related to the opposing H3K4me3 profile rather than to the CpG density that classically defines CpG islands (>200bp, GC content >50%, observed/expected ration >0.6), with the exception of the *GNAS-XL* DMR. This maternally methylated region was thought to be a single regulatory unit, however our WGBS and Infinium array data clearly show that it is two separate DMRs, partitioned by a ~ 200 bp interval of hypermethylation with the centromeric *GNAS-AS1* (previously known as *NESP*-AS) promoter showing co-enrichment for H3K4me3 and DNA methylation, while the *GNAS-XL* side lacks this permissive histone modification (Fig. 3A).

Further interrogation of this dataset identified two DMRs associated with multiple promoters with a gradient effect across the CpG-rich sequences. The *GNAS*/*GNAS EX1A* CpG island (CpG island 320 in Fig. 3A) is unmethylated on one side, coinciding with H3K4me3, whilst the other is differentially methylated with abundant H3K4me3 and meDIP reads. This pattern was also observed at the bidirectional *HTR5A*/*HTR5A-AS1* promoter in brain (Fig. 3B), a tissue where these transcripts are most abundant.

Tissue-specific dynamics of imprinted DMRs

The WGBS analysis in leukocytes, brain and liver confirmed that the extent of allelic methylation at the imprinted DMRs, as defined by the size of the intermediately methylated interval, is highly similar in these somatic tissues (Fig. 1 and 4; Table 1). However, some regions were drastically different in the placenta.

By comparing the placental WGBS profile with Infinium β-values for placentae and hydatidiform moles, we observe that the DMRs associated with the maternally methylated *PEG10* and the paternally methylated *H19* are significantly larger in placenta than somatic tissues. Using standard bisulphite PCR and sequencing, we confirm that the somatically unmethylated *SGCE* promoter, immediately adjacent to the differentially methylated *PEG10* promoter is methylated on the maternal allele in placenta, while the maternal allele overlapping the *H19* gene body is demethylated (Fig. 4B).

In addition to identifying extended DMRs in the placenta, we also observe complex tissue-specific methylation between somatic tissues and placenta. For example, the *NNAT* and *GNAS-AS1* DMRs, which are maternally methylated in somatic tissue, exhibit hypermethylation in both placenta and hydatidiform mole. Subsequent bisulphite PCR confirmed that these regions are fully methylated in the placenta (Supplemental Fig. S4). Methylation profiling at the *MIR512-1* cluster (also known as *C19MC*)-*ZNF331* locus on chromosome 19 has previously disclosed that the promoter of the pri-miRNA for this miRNA cluster is maternally methylated in placenta, but fully methylated in somatic tissues (Noguer-Dance et al. 2010). We confirm that the *MIR512-1* DMR is unmethylated in hydatidiform moles compared to the partially methylated profile in placenta with placental WGBS revealing that the DMR is ~5 kb in size incorporating the promoter CpG island (CpG island 86 in Fig. 4C). However, we notice that the CpG island (CpG island 83 in Fig. 3C) associated

Downloaded from genome.cshlp.org on November 14, 2026 . Published by Cold Spring Harbor Laboratory Press

with *ZNF331* isoform-3 is hypermethylated on both parental alleles in placenta but is a maternally methylated DMR in somatic tissues. These methylation states dictate complex allelic expression at this locus, with restricted placental-specific paternal expression of the *MIR512-1* pri-miRNA, which does not extend to the *MIR371/2* cluster, and reciprocal imprinting of *ZNF331* (Fig. 4C; Supplemental Table S2).

Novel placental-specific DMRs associated with paternally expressed transcripts

Based on the complex methylation profiles described above, we next investigated if more unknown imprinted DMRs exist solely in placental tissues, as highlighted by the *MIR512-1* and *GPR1-AS* DMRs (Noguer-Dance et al. 2010; Kobayashi et al. 2013). We performed a screen for partially methylated regions present solely in our placenta WGBS dataset using our sliding window approach (0.25< mean of 25 CpG +/- 2 SD<0.75). This identified 722 windows, of which 520 mapped to CpG islands. These results confirm that placental-derived DNA is significantly less methylated when compared to other tissues (Schroeder et al. 2013) and that this lower methylation genome-wide is not restricted to repetitive elements as previously described (Ehrlich et al. 1982; Fuke et al. 2004) but occurs across a large portions of the genome.

Of these partial methylated placenta domains identified by WGBS, 44 regions were ~50% methylated in placenta with extreme methylation in hydatidiform mole using the Infinium array (average β-values for 3 consecutive probes >0.8 indicative of paternal methylation or <0.2 for maternal methylation), and which showed no evidence of allelic methylation in somatic tissues. Using standard bisulphite PCR we assessed the allelic methylation profile of all regions in placental DNA samples. This revealed that the promoters of *N4BP2L1, DCAF10, PDE4D, FAM196A, RGMA, AGBL3, MCCC1, ZC3H12C, DNMT1, AIM1, ZNF396, FAM20A, GLIS3* and *LIN28B* are methylated on the maternal allele (Fig. 4D; Supplemental Fig. S5; Supplemental Table S2). In addition, we identified a 2.8 kb region of intermediate methylation overlapping an alternative promoter of the paternally expressed *ZFAT* gene in the placental WGBS dataset (Supplemental Fig. S5). Using allelic-specific bisulphite PCR, we confirm that the methylation is confined to the maternal chromosome at this locus. To determine if these regions of maternal methylation influence transcription, allelic RT-PCR experiments were carried out. Paternal expression of eight of these genes was verified, with biallelic expression in somatic tissues (Fig. 4D; Supplemental Fig. S5; Supplemental Table 2), consistent with recent allelic expression screens in term placenta (Yuen et al. 2011; Barbaux et al. 2012).

Mammalian conservation of novel imprinted domains

To determine if the previously unrecognised imprinted domains are conserved throughout evolution, we assessed their allelic methylation and expression in mice, using reciprocal cross between mouse strains. Bisulphite PCR targeting of orthologous regions failed to identify evidence of differential methylation in embryonic day E9.5-14.5 embryos or extra-embryonic tissues. Subsequent allelic RT-PCRs revealed that all murine transcripts orthologous to the novel ubiquitous and placental-specific imprinted transcripts are expressed equally from both parental alleles when detected (Supplemental Fig. S6 & S7). This suggests that these new imprinted domains arose less than ~80 million years ago after the divergence of mice and humans or that selection pressures over this period have resulted in a loss of imprinted regulation of these genes in mice. It has been previously reported that imprinting in the placenta differs between human and mouse, mainly due to the lack of imprinting of genes which require repressive histone modifications for allelic

Downloaded from genome.cshlp.org on November 14, 2026 . Published by Cold Spring Harbor Laboratory Press

silencing in humans (Monk et al. 2006). Contrary to previous reports, our results show that humans have evolved more loci being subject to this form of transcriptional regulation in placenta due to the evolutionary acquisition of loci with parent-of-origin methylation. This is endorsed by the low discovery rate of novel imprinted transcripts in RNA-seq screens of mouse placenta (Okae et al. 2011).

Differential methylation at ubiquitously imprinted loci and placental-specific domains may differ in their gametic origin

An essential step towards understanding the establishment of the germline imprint signal is to determine if the parent-of-origin methylation observed in somatic tissues is derived from the germline. Determining the methylation profiles in human gametes and during the early pre-implantation stages of embryonic development is technically and ethically challenging. To circumvent these difficulties, we have used a combination of mature gametes and *in vitro* models to represent human gametes of both sexes and pre-implantation embryos. For analysis during gametogenesis in males, we used mature sperm. We compared publically available WGBS datasets from sperm and human embryonic stem (hES) cells that represent the inner cell mass cells of the blastocysts (Lister et al 2009; Molaro et al. 2011) with our own Infinium array profiles for sperm, parthenote-derived hES cells lines (phES) and hES cell lines generated from both six-cell blastomeres (Val10B) and inner cell mass of blastocysts (SHEF cell lines). Despite the phES cell lines having undergone reprograming during blastocyst development, they have previously been shown to retain maternal hypermethylation at the limited imprinted loci assessed, suggesting they are ideal surrogates for assessing the methylation profiles of imprinted DMRs in mature oocytes (Mai et al. 2007; Harness et al. 2011).

A comparison of Infinium β-values between sperm and phES cells for the human sequences orthologous to the mouse germline DMRs (Kobayashi et al. 2012) revealed that 19/22 are conserved. The novel ubiquitous DMRs we identify are also hypermethylated in phES cells and unmethylated in sperm suggesting that the majority of imprinted DMRs, with the exception of *IGF1R*, are primarily marked in the gametes (Fig. 5A; Supplemental Fig. S8). In addition we confirm that the IG-DMR within the chromosome 14 domain is >80-90% methylated in the sperm WGBS dataset, in line with previous reports (Geuns et al. 2007). We were particularly intrigued to observe that all placental-specific DMRs, with the exception of *ZFAT, GPR1-AS* and *MIR512-1*, do not inherit methylation from the gametes, and are devoid of methylation in hES cells (Fig. 5A). These data provide preliminary evidence to suggest that following gametogenesis parental alleles at some loci retain a non-equivalency that is not associated with DNA methylation. Therefore, in the female germline, as represented by the phES cells, a subset of imprinted loci retain their identity in the absence of methylation, suggesting that additional epigenetic mechanisms mark these regions for maternal methylation during trophoblast differentiation (Fig. 5A).

For the majority of DMRs for which allelic methylation was observed in the somatic tissues (80%), the genomic interval showing methylation differences between sperm and phES cells is larger than the allelic DMRs in hES cells and somatic tissues (Fig. 5B, C). In the case of maternally methylated DMRs, we observe that these regions are flanked by fully methylated intervals in both gametes, and that these DMRs are observed as regions devoid of methylation in the sperm genome. Interrogation of ChIP-seq datasets for nucleosomes containing the histone modifications revealed that the majority of unmethylated DMR regions in sperm are

Downloaded from genome.cshlp.org on November 14, 2026 . Published by Cold Spring Harbor Laboratory Press

enriched for H3K4me3 containing nucleosome fractions. Our analysis indicates that the size of the unmethylated region in sperm is therefore associated with nucleosome occupancy, rather than protamines. Notably, the maternally methylated germline DMR overlapping the *NNAT* promoter is ~4 kb, as defined by full methylation in phES cell and the H3K4me3 enriched DNA unmethylated region in sperm. This regions contracts to an ~1.5 kb region of maternal methylation after pre-implantation reprogramming as represented by blastocyst-derived hES cells and somatic tissue profiles (Fig. 5C and Supplemental Fig. S9A showing the contraction at the *NAP1L5* locus). Such resizings are also observed in mouse (Tomizawa et al. 2011), suggesting that imprinted DMRs are not totally protected from genome-wide demethylation during the oocyte to embryo transition. We speculate that the larger regions of differential methylation dictated by the gametes, in combination with protective factors, ensure they survive reprogramming.

In addition, we also observe other subtle differences in germline-derived methylation profiles. For example, the two sides of the *GNAS-XL* DMR that we show have independent H3K4 methylation profiles from each other behave differently in the germline, with *GNAS-AS1* side being a somatic DMR only, but the *GNAS-XL* side being methylated in phES cells and hypomethylated in sperm (Supplemental Fig. S4). Lastly, we identified a dynamic relocalization of methylation at the *FAM50B* DMR during pre-implantation development. The 1.2 kb promoter of this imprinted retrogene is methylated on the maternal allele in somatic tissues but is completely unmethylated in phES cells and hES cells derived from 6-cell embryos, and has been shown to be unmethylated in sperm (Nakabayashi et al. 2011). However, we do find allelic methylation is conferred during pre-implantation development, at a point between the six-cell stage and blastocyst development. In fact, the ~1 kb regions flanking the promoter (labelled 1 and 3 in Supplemental Fig. S9B) show strongly opposing methylation profiles with the sperm being unmethylated and phES cells methylated, which then becomes fully methylated on both alleles immediately after fertilization, leaving allelic methylation over the promoter itself.

Discussion

Differentially methylated regions between the parental alleles are essential for genomic imprinting and development. In this study, we have performed a comprehensive survey of methylation in various human tissues, uncovering all known imprinted DMRs as well as 21 novel loci, which we demonstrate wherever possible regulate imprinted transcription. Our present work demonstrates that the human genome contains a significantly larger number of regions of parent-of-origin methylation than previously thought. The identification of imprinted domains has traditionally been performed in mouse by utilizing gynogenetic and androgenetic embryos, mice harboring regions of uniparental disomies, or highly polymorphic inbred strains (Cooper et al. 2010). These embryos have been subjected to expression-based screens including RNA-seq (Gregg et al. 2010; Okae et al. 2011) and genome-wide methylation techniques (Hayashizaki et al. 1994; Kelsey et al. 1999; Hiura et al. 2010). By relying on the confirmation of evolutionarily conserved expression of the human orthologues, imprinted genes specific to higher primates and humans will have been missed. We have utilized high-throughput bisulphite analysis from *in vitro* models of gametes and early embryos, somatic and placental DNA to characterize the developmental dynamics of imprinted methylation coupled with allelic expression analysis of nearby transcripts. This analysis reveals that 30 regions of parentally inherited differential methylation are observed in humans but not mice. Conversely,

Downloaded from genome.cshlp.org on November 14, 2026 . Published by Cold Spring Harbor Laboratory Press

we also show that the DMRs associated with *Cdkn1c*, *Rasgrf1*, the *Igf2r* promoter, *Impact*, *Slc38a4* and *Zrsr1* (previously known as *U2af1-rs1*) imprinted transcripts in mouse do not exhibit allelic methylation in humans (Xie et al. 2012).

Recently a novel mechanism has been described in which differences in germline methylation can give rise tissue-specific DMRs in mouse (Proudhon et al. 2012). The *Cdh15* DMR inherits methylation from the oocyte and maintains this parental allelic methylation during *in utero* development and in adults with the exception that the paternal allele gains methylation in various brain regions. Therefore the intragenic *Cdh15* DMR is conserved during adulthood, but in a tissue-specific manner. In humans, the *CDH15* locus does not exhibits allelic DNA methylation any tissue (data not shown), suggesting that this tissue-specific methylation profile might be limited to mice. We cannot rule out the existence of temporally regulated tissue-specific imprinted DMR in humans, since our samples were derived from adults, and therefore any imprinted DMRs specific to the fetal period would be missed.

Our study reveals the power of combining WGBS and Infinium HumanMethylation450 BeadChip arrays to identify novel imprinted DMRs. We have previously combined reciprocal genome-wide UPD samples and the Infinium HumanMethylation27 BeadChip arrays to identify imprinted loci (Nakabayashi et al. 2011). All new regions of ubiquitous imprinted methylation identified in the current screen are associated predominantly with type II Infinium probes and were not present on previous array platforms. Of the placental-specific DMRs only those associated with *DNMT1, AIM1* and *MCCC1* have been previously described (Yuen et al., 2011, Das et al., 2013). Intriguingly the somatic promoter of *Dnmt1* is differentially methylated between sperm and oocytes but is lost during pre-implantation development (Smallwood et al. 2011, Kobayashi et al. 2012). Two of these placental-specific DMRs are associated with type I Infinium probes and were previously discovered using the Infinium HumanMethylation27 BeadChip arrays with DNA derived from diandric and digynic triploid placental samples (Yuen et al. 2011).

Our data provide the first direct evidence in humans that the differential methylation associated with imprinted genes is dynamically regulated upon fusion of the gametes at fertilization. Most maternally methylated DMRs are surrounded by regions of complete methylation in both gametes, and as in mice, the DMRs are clearly observed as unmethylated islands in the sperm genome. These unmethylated intervals are often more extensive in sperm compared to somatic tissues, suggesting resizing occurs during embryonic transition. It was recently reported that nucleosomes are retained at specific functional regions in sperm chromatin and are refractory to protamine exchange (Hammoud et al. 2009). These sperm-derived histones are enriched for H3K4me3, a permissive modification that is mutually exclusive with DNA methylation, implicating these H3K4me3 regions in the maintenance of the unmethylated state in the male germline.

Imprints are distinguishable from other forms of gametic methylation as they survive the reprogramming that initiates immediately upon fertilization (Smallwood et al. 2011; Kobayashi et al. 2013; Proudon et al. 2012). By comparing the profiles of sperm, phES and conventional hES cells along with somatic tissues, we present evidence that most maternally methylated DMRs are not completely refractory to reprogramming, as highlighted by the substantial resizing of the paternally derived unmethylated alleles. These data are consistent with the notion that the cores of imprinted DMRs are protected from Tet-associated demethylation by recruiting heterochromatic factors such as ZFP57 and DPPA3 (also known as STELLA or PGC7)(Li et al. 2008; Nakamura et al. 2007). Similar mechanisms could also act to

Downloaded from genome.cshlp.org on November 14, 2026 . Published by Cold Spring Harbor Laboratory Press

protect the core of the unmethylated paternal alleles from methylation.

A search for the mouse ZFP57 recognition sequence (TGCC^{met}GC) identified numerous binding sites within the ubiquitous imprinted DMRs that maybe involved in protecting methylation during pre-implantation reprogramming (Quenneville et al. 2011). It is currently unknown if this hexonucleotide motif is bound by ZFP57 in human cells, but patients with mutated ZFP57 lack DNA binding capacity in *in vitro* EMSA studies (Baglivo et al. 2013).

There is significantly less ZFP57 sequence motifs in the placental-specific DMRs compared to the ubiquitous DMRs that inherit methylation from the germline ($p<0.05$ Student's t-test), with 14/17 placental-specific DMRs being unmethylated and not associated with H3K9me3 in hES cells (Supplemental Fig. S10). These data further support our hypothesis that a novel imprinting mechanism occurs in the placenta, which is one of the first examples of methylation independent epigenetic inheritance in mammals. In support of our our observations, Park and colleagues (Park et al. 2004) generated a *H19* ICR knock in at the *Afp* locus which was *de novo* methylated around gastrulation, implying that that *H19* ICR is differentially marked in the gametes by a mechanism other than methylation. However, it is unknown if this mechanism also occurs at the endogenous *H19* locus. In our examples of placental-specific DMRs the epigenetic mark inherited from the oocyte is currently unknown, but must be recognised by the *de novo* methylation machinery during early trophoblast differentiation, since we observe maternal methylation in term placenta. Certain histone methylation states are reported to recruit DNMTs (Zhang et al. 2010; Dhayalan et al. 2010). Since various post-translational modifications of histone tails have been shown to be present at imprinted loci, specifically in the placenta independent of DNA methylation (Umlauf et al. 2004; Monk et al. 2006), we are led to suggest one inviting hypothesis, that a histone modification confers the "imprint" at these novel placental-specific imprinted loci. Alternatively, the DNMTs maybe recruited to these loci by a specific, yet to be identified, transcription factor expressed during early trophoblast differentiation.

In line with other well characterised imprinted genes in the placenta, the placental-specific imprinted transcripts may also exert supply and demand forces between the developing fetus and mother, ultimately influencing fetal adaptation *in utero*, which if disrupted may have long-term consequences on health many decades after delivery (Constância et al. 2004). Our observation of imprinting of the somatic promoter of *DNMT1* in placenta may therefore assist in this process. In addition, numerous studies have also suggested that children born as a result of assisted reproductive technologies (ART), including ovarian stimulation, *in vitro* fertilization and intracytoplasmic sperm injections, have a higher risk of diseases with epigenetic aetiologies including imprinting disorders (Amor et al. 2008). In a clinical context, the placenta-specific imprinted loci may be prone to epigenetic instability during ART, as the first differentiation step that results in the trophectoderm occurs when the developing blastocysts are in culture.

By utilizing genome-wide methylation profiling at base-pair resolution we have catalogued regions of parentally inherited methylation associated with imprinted regions and highlighted all difference between somatic and placental tissues. Further studies of these loci will provide insight into the causes of epigenetic aberrations associated with imprinting disorders and may be relevant to the epigenetic causes of common diseases.

Downloaded from genome.cshlp.org on November 14, 2026 . Published by Cold Spring Harbor Laboratory Press

Methods

Tissue samples and cell lines.

Peripheral blood was obtained from healthy volunteers or from umbilical cord of newborns for which we obtained matched placental biopsies. These samples were collected at Hospital St Joan De Deu (Barcelona, Spain) and the National Center for Child Health and Development (Tokyo, Japan). All placenta-derived DNA samples were free of maternal DNA contamination biased on microsatellite repeat analysis. The brain samples were obtained from BrainNet Europe/Barcelona Brain Bank. Ethical approval for this study was granted by the Institutional Review Boards at the National Center for Child Health and Development (project 234), Saga University (21-5), Hamamatsu University School of Medicine (23-12), Hospital St Joan De Deu Ethics Committee (35/07) and Bellvitge Institute for Biomedical Research (PR006/08). Written informed consent was obtained from all participants.

The hES (SHEF 3, 5, 6 and Val10B) and parthenogenetically activated oocyte (LLC6P, LLC7P, LLC8P and LLC9P) cell lines were used since they were epigenetically stable at imprinted loci (with the exception of *NNAT* LOM and *GNAS* GOM in LLC7P; LOM of *PEG3* in Val10B; GOM of *MCTS2* in SHEF3) and grown as previously described (Harness et al., 2011). Ethical approval for the study of these cells was granted by Bellvitge Institute for Biomedical Research Ethics Committee (PR096/10) and Comité Ético de Investigación Clínica (CEIC) del Centro de Medicina Regenerativa de Barcelona-CMR[B] (28/2012) and complied with the legal guidelines outlined by the Generalitat de Catalunya El conseller de Slaut.

Wild type mouse embryos and placentae were produced by crossing C57BL/6 (B) with *Mus musculus molosinus* (JF1) or *Mus musculus castaneous* (C) mice. Mouse work was approved by the Institutional Review Board Committees at the National Center for Child Health and Development (approval number A2010-002). Animal husbandry and breeding were conducted according to the institutional guidelines for the care and the use of laboratory animals. DNA and RNA extractions and cDNA synthesis were carried out as previously described (Monk et al., 2006).

Characterization of the genome-wide UPD samples.

Genomic DNA was isolated from two previously described genome-wide paternal UPD cases with BWS features (Romanelli et al., 2011) and two newly identified individuals, at Saga University, as well as one genome-wide maternal UPD with a SRS phenotype (Yamazawa et al., 2010). Each of these cases had undergone extensive molecular characterization to confirm genome-wide UPD status and the extent of mosaicism. We used DNA isolated from lymphocytes as these samples had minimal contamination of the biparental cell lines. The genome-wide pUPD samples had 9, 11, 9 and 2 % biparental contribution, whereas the genome-wide SRS sample had 16%. In addition, four hydatidiform moles were collected by the National Center for Child Health and Development.

Genome-wide methylation profiling.

We analysed 6 publically available methylomes, including those derived from CD4+ lymphocytes (GSE31263)(Heyn et al., 2012), brain (GSM913595) (Zeng et al., 2012) the H1 hES cell line (GSM432685, GSM432686, GSM429321, GSM429322, GSM429323) and sperm (GSE30340). In addition we generated 3 additional tissue methylomes using WGBS for brain, liver and placenta. WGBS libraries were generated as described previously (Heyn et al., 2012).

Downloaded from genome.cshlp.org on November 14, 2026 . Published by Cold Spring Harbor Laboratory Press

We also generated methylation datasets using the Illumina Infinium HumanMethylation450 BeadChip arrays, which simultaneously quantifies ~2% of all CpG dinucleotides. Bisulphite conversion of 600 ng of DNA was performed according to the manufacturer's recommendations for the Illumina Infinium Assay (EZ DNA methylation kit, ZYMO, Orange, CA). The bisulphite-converted DNA was used for hybridization following the Illumina Infinium HD methylation protocol at genomic facilities of the Cancer Epigenetics and Biology Program (Barcelona, Spain) or the National Center for Child Health and Development. The resulting data for the genome-wide UPDs (4x pUPD, 1x mUPD), 2 brain, 1 liver, 1 muscle, 1 pancreas, 2 sperm, 4 hydatidiform moles, 4 term placentae, 4 phES cell lines and the 4 hES lines have been deposited in the GEO database with the accession number GSE52578. In addition we used 3 leukocyte datasets from GSE30870.

Data filtering and analysis.

WGBS: The sequence reads were aligned to either strand of the hg19 reference genome using a custom computational pipeline (autosomal CpGs with at least 5 reads: brain sample- 190,314,071 aligned unique reads, 83% coverage; liver sample- 778,733,789 aligned unique reads, 96.6% coverage; placenta sample- 319,362,653 aligned unique reads, 89.6% coverage). The methylation level of each cytosine within CpG dinucleotides was estimated as the number of reads reporting a C, divided by the total number of reads reporting C or T. For the identification of intermediately methylated regions associated with imprinted DMRs we performed a sliding window approach in which the methylation of 25 CpGs was averaged after filtering for repetitive sequences. The location of these sequences was taken from the UCSC sequence browser. An interval was considered partially methylated if the average methylation was $0.25 <$ mean +/- 1.5 SD< 0.75.

Illumina Infinium HumanMethylation 450 BeadChip array: Before analysing the data, we excluded possible sources of technical biases that could influence results. We applied signal background subtraction and inter-plate variation was normalized using default control probes in BeadStudio (version 2011.1_Infinium HD). We discarded probes with a detection p-value >0.01. We also excluded probes that lack signal values in one or more of the DNA samples analysed. In addition we discarded 16,631 probes as they contained SNPs present in more than 1% of the population (dbSNP 137). Lastly, prior to screening for novel imprinted DMRs we excluded all X chromosome CpG sites. In total we analysed 442,772 probes in all DNA samples. All hierarchical clustering and β-value evaluation was performed using the Cluster Analysis tool of the BeadStudio software.

In-house R-package scripts were used to evaluate the average methylation of 3 contiguous Infinium probes. To identify regions with potential allelic methylation we screened the reciprocal genome-wide UPDs for 3 consecutive probes with an average β-value difference greater than of 0.3 (Limma linear model $p<0.05$):

$$\left| \frac{1}{3}\sum_{n=0}^{2} pUPDs_n - \frac{1}{3}\sum_{n=0}^{2} mUPD_n \right| > 0.3$$

With the condition that the average of 3 consecutive probes for the normal leukocytes is between the values for the reciprocal genome-wide UPDs:

Downloaded from genome.cshlp.org on November 14, 2026 . Published by Cold Spring Harbor Laboratory Press

$$\begin{cases} if\ \frac{1}{3}\sum_{n=0}^{2} pUPDs_n > \frac{1}{3}\sum_{n=0}^{2} mUPD_n\ then\ \frac{1}{3}\sum_{n=0}^{2} pUPDs_n > \frac{1}{3}\sum_{n=0}^{2} Leukocytes_n > \frac{1}{3}\sum_{n=0}^{2} mUPD_n \\ if\ \frac{1}{3}\sum_{n=0}^{2} mUPD_n > \frac{1}{3}\sum_{n=0}^{2} pUPDs_n\ then\ \frac{1}{3}\sum_{n=0}^{2} mUPD_n > \frac{1}{3}\sum_{n=0}^{2} Leukocytes_n > \frac{1}{3}\sum_{n=0}^{2} pUPDs_n \end{cases}$$

The final condition was that the average of 3 consecutive probes for normal leukocytes is within the 0.25-0.75 intermediate methylation range:

$$0.25 > \frac{1}{3}\sum_{n=0}^{2} Leukocytes_n > 0.75$$

Genotyping and imprinting analysis.
Genotypes of potential SNPs identified in the UCSC hg19 browser were obtained by PCR and direct sequencing. Sequence traces were interrogated using Sequencher v4.6 (Gene Codes Corporation, MI) to distinguish heterozygous and homozygous samples. Heterozygous sample sets were analysed for either allelic expression using RT-PCR or bisulphite PCR, incorporating the polymorphism within the final PCR amplicon so that parental alleles could be distinguished (for primer sequence see Supplemental Table S3).

Bisulphite PCR.
Approximately 1 µg DNA was subjected to sodium bisulphite treatment and purified using the EZ DNA methylation-Gold kit (ZYMO, Orange, CA) and was used for all bisulphite PCR analysis. Approximately 2 ul of bisulphite converted DNA was used in each amplification reaction using Immolase Taq polymerase (Bioline) at 35-45 cycles and the resulting PCR product cloned into pGEM-T easy vector (Promega) for subsequent subcloning and sequencing (for primer sequence see Supplemental Table S3). For the confirmation of an imprinted DMR we analysed a minimum of three heterozygous samples and where possible two different tissues.

Chromatin immunoprecipitation (ChIP).
We analysed publically available H3K4me3 ChIP-seq and meDIP-seq datasets, including those derived from lymphocytes (GSM772948, GSM772836, GSM772916, GSM543025, GSM613913), brain (GSM806943, GSM806935, GSM806948, GSM669614, GSM669615) and the H1 hES cell line (GSM409308, GSM469971, GSM605315, GSM428289, GSM456941, GSM543016). For H3K9me3 in hES cells, we used GSM450266. In addition we used the sperm ChIP-seq dataset for H3K4me3 as a direct measure of nucleosome occupancy (GSM392696, GSM392697, GSM392698, GSM392714, GSM392715, GSM392716)(Hammoud et al., 2009).

The confirmation of allelic H3K4me3 in leukocytes or lymphoblastoid cell lines was performed as previously described (Iglesias-Platas et al., 2013). Briefly, 100 µg of chromatin was used for immunoprecipitation reaction with Protein A agarose/salmon sperm DNA (Millipore, 16-157) and a H3K4me3 (07-473 Millipore). Each ChIP was performed in triplicate alongside a mock immunoprecipitation with an unrelated IgG antiserum and a 1% fraction of the input chromatin was extracted in parallel. Levels of immunoprecipitated chromatin at each specific region were determined by qPCR using SYBR Green (Applied Biosystems) carried out on the Applied Biosystems 7900 Fast real-time PCR system (for primer sequence see Supplemental Table S3). Each PCR was run in triplicate and protein binding was

Downloaded from genome.cshlp.org on November 14, 2026 . Published by Cold Spring Harbor Laboratory Press

quantified as a percentage of total input material.

Data Access.
This data has been submitted to the Gene Expression Omnibus (GEO) and has been assigned the accession number GSE52578.

Acknowledgements
We would like to thank S. Morán at PEBC-IDIBELL for performing the methylation array hybridization, S. Sayols and H. Heyn for bioinformatics assistance. We are also grateful to P. Arnaud and J. Frost for stimulating discussions and helpful comments. This work was partially funded by grants from the Fundació La Marató de TV3 (grant number 101130 to D.M and P.L); Spanish Ministerio de Educacion y Ciencia (BFU2011-27658 to D.M); JST/CREST and the Health and Labour Sciences Research Grant (Nanbyo-Ippan-003) to K.H; the Ministry of Education, Culture, Sports, Science, and Technology of Japan (#22249010) and the Grant of National Center for Child Health and Development (#24-3) to K.N. D.M is a Ramon y Cajal research fellow. Finally, we would like to thank all the patients and their families for participating in this project.

Disclosure
All authors declare no conflict of interest.

Figure legends

Figure 1. Identification of known imprinted DMRs on the Infinium array platform.
(A) Circular karyotype showing the difference of methylation for three consecutive probes for reciprocal UPD leukocyte samples. Red dots correspond to a minimal difference of 0.3 Infinium probe β-values (>30% absolute methylation value) for regions with maternal methylation and blue dots for paternal methylation. Known DMRs are indicated. (B) Heatmap of the Infinium probes located within known imprinted DMRs in reciprocal genome-wide UPD samples and various somatic tissues. (C) WGBS and Infinium array methylation profiles of the *ZNF597* locus with bisulphite PCR confirmation of the novel maternally methylated DMR and its position in relation to the somatic paternally methylated promoter region. Vertical grey lines in the WGBS tracks represent the mean methylation value for individual CpG dinucleotides calculated from multiple data sets, with the light grey lines representing the mean + standard deviation. Infinium methylation values for normal tissues are represented by black dots, with values for the genome-wide UPDs (average pUPD in blue and mUPD in red) superimposed on the leukocyte methylation track. The error bars associated with the Infinium array probes present the standard deviation of multiple biological samples. The PCR confirmation in placenta, kidney and leukocyte-derived DNA was performed on heterozygous samples. Each circle represents a single CpG dinucleotide on a DNA strand, (●, methylated cytosine; o unmethylated cytosine). Each row corresponds to an individual cloned sequence.

Figure 2. Identification and characterization of allelic methylation and expression of novel imprinted loci.
Circular karyotype showing the position of common regions of intermediate methylation in the leukocyte, brain and liver WGBS datasets as identified a 25 CpG sliding window approach (0.25<mean ± 1.5 SD<0.75) Red ticks represent site of

Downloaded from genome.cshlp.org on November 14, 2026 . Published by Cold Spring Harbor Laboratory Press

intermediate methylation common to all tissues, where as black ticks identify those present in only one or two pair-wise comparisons. The position of known imprinted DMRs are shown. (B) Identification of a novel maternally methylated DMR within the *WDR27* locus by WGBS and Infinium array analysis. Vertical grey lines in the WGBS tracks represent the mean methylation value for individual CpG dinucleotides calculated from multiple data sets, with the light grey lines representing the mean + standard deviation. Infinium methylation values for normal tissues are represented by black dots, with values for the genome-wide UPDs (average pUPD in blue and mUPD in red) superimposed on the leukocyte methylation track. The DMR was confirmed using standard bisulphite PCR on heterozygous DNA samples and orchestrates paternal expression of *WDR27* isoform 2. The asterisk (*) in the sequence traces shows the position of the polymorphic base. (C) Imprinting of *ERLIN2* isoform 1 in leukocytes as a consequence of retrotransposition of X chromosome-derived *CXorf56* pseudogene into the locus.

Figure 3. H3K4me3 chromatin profile and DNA methylation at imprinted loci. (A) Map of the human *GNAS* locus on chromosome 20 with the H3K4me3 and meDIP signatures in brain and leukocytes at the DMRs identified in the WGBS and Infinium array analysis. Infinium methylation values for normal leukocytes (black dots), with values for the genome-wide pUPD (blue) and mUPD (red) superimposed on the leukocyte WGBS track. Similarly Infinium methylation values for two normal brain samples shown as black and grey dots. The two shades of grey peaks in the meDIP and ChIP-seq panels represent two independent biological replicates compared to input (black peaks). The bars under the CpG islands, as identified in the UCSC sequence browser, show the location of the bisulphite PCR amplicons. (B) The gradient DMR identified at the *HTR5A* promoter. The samples used for the WGBS, Infinium array and ChIP are the same as in (A). The independent methylation patterns either side of the bi-directional promoter interval was confirmed using standard bisulphite PCR and sequencing. (C) Allelic ChIP for H3K4me3 reveals predominant enrichment of this histone modification on the unmethylated allele of the *H19* ICR, *SNURF ICR, NNAT* and *MCTS2* DMRs. The asterisk (*) in the sequence traces shows the position of the polymorphic base

Figure 4. The methylation profiles of imprinted loci in placenta compared to somatic tissues. The placenta- and leukocyte-derived WGBS and Infinium array profiles at the (A) *PEG10* and (B) *H19* loci. Infinium methylation values for normal leukocytes (black dots), with values for the genome-wide pUPD (blue) and mUPD (red) superimposed on the leukocyte WGBS track. Similarly Infinium methylation values for normal placenta (black dots) and hydatidiform mole (blue dots) are overlaid on the placental WGBS track. The error bars associated with the Infinium array probes represent the standard deviation of multiple biological samples. Bisulphite PCR analysis was used to confirm the tissue-specific methylation profiles. (C) Complex tissue-specific allelic methylation and expression patterns at the *ZNF331-MIR512* cluster locus on chromosome 19. The *ZNF331* sequence traces represent the RT-PCR products from leukocytes, whereas both *MIR512-1* cluster and *MIR371/2* are from placenta. (D) A placental-specific imprinted DMR identified using the placenta-derived WGBS and Infinium array datasets. The methylation profiles were confirmed using standard bisulphite PCR on heterozygous DNA samples with allelic RT-PCR performed on placental biopsies. The results confirm

Downloaded from genome.cshlp.org on November 14, 2026 . Published by Cold Spring Harbor Laboratory Press

that the region of maternal methylation overlapping the *AGBL3* promoter dictates paternal expression of this gene in placenta.

Figure 5. Methylation in gametes, hES cells and somatic tissues. (A) Heatmaps for Infinium probes mapping within all ubiquitous (left) and placental-specific (right) imprinted DMRs in sperm and phES cells reveal the germline acquisition of methylation. (B) Methylation contour plots from WGBS datasets for all maternally methylated DMRs reveals that the extent of the intermediately methylated regions associated with imprinted DMRs are extremely consistent between somatic tissues and significantly larger in sperm. (C) Methylation profiles at the *NNAT* DMR determined by WGBS, Infinium array and meDIP-seq datasets in leukocytes, sperm, phES cells and hES cells, along with the H3K4me3 ChIP-seq reads for hES cells and sperm. The grey and black dots in the second panel represent Infinium probe methylation in hES cell lines derived from six-cell blastomeres (Val10B) and blostocytes (SHEF5), respectively. The gametic WGBS methylation profile is derived from sperm, with Infinium probe methylation values for sperm and phES cells represented by blue and red dots. The graphic shows the extent of the differentially methylated regions in somatic tissues and between sperm and phES cells. The error bars associated with the Infinium array probes represent the standard deviation of the 2 sperm samples and 4 independent phES cells cell lines. The H3K4me3 ChIP-seq data is from sperm. The methylation profiles were confirmed using standard bisulphite PCR and sequencing.

Table 1.
Location of parent-of-origin methylation identified in this study. The extent of imprinted methylation is defined by the size of the intermediately methylated region from the lymphocyte (for ubiquitous DMRs) and placenta (for placental-specific DMRs) WGBS dataset.

Supplemental Figure S1.
Sample comparisons between WGBS and Illumina Infinium arrays.
Linear regression analysis of individual CpG sites as revealed by the WGBS compared to corresponding Infinium probe β-values for blood, placenta, sperm, hES cells, brain and liver. The results are highly correlative when the same DNA samples are compared (blood, brain and placenta), and similar for DNA from different samples of the same tissue origin (sperm, liver and hES cells). The red and blue data points represent the probes mapping to known maternally and paternally methylated DMRs respectively.

Supplemental Figure S2.
Genome-wide methylation profiling identifies novel allelic DMRs within known imprinted domains.
(A) A map of the *SNRPN* domain on human chromosome 15, showing the position of the known imprinted transcripts and CpG islands with the methylation profile obtained using leukocyte-, brain- and liver-derived WGBS and Infinium array datasets. Vertical grey lines in the WGBS tracks represent the mean methylation value for individual CpG dinucleotides calculated from multiple data sets, with the light grey lines representing the mean + standard deviation. Infinium methylation values for normal tissues are represented by black dots, with values for the genome-wide UPDs (average pUPD in blue and mUPD in red) superimposed on the leukocyte

Downloaded from genome.cshlp.org on November 14, 2026 . Published by Cold Spring Harbor Laboratory Press

methylation track. The methylation profiles were confirmed using standard bisulphite PCR and sequencing in brain and leukocyte DNA samples. Each circle represents a single CpG dinucleotide on a DNA strand, (●, methylated cytosine; O unmethylated cytosine). Each row corresponds to an individual cloned sequence. (B) The tissue-specific intergenic DMR identified within the *MEG8* gene on chromosome 14 as identified by combined WGBS and Infinium array analysis in leukocytes, brain and liver. The DMR was subsequently confirmed by bisulphite PCR and sequencing. (C) The novel DMR within CpG island 30 overlaps exon 2 of the *DIRAS3* transcript, in addition to the known promoter DMR. The WGBS and Infinium array analysis confirm that both regions are ubiquitous DMRs, which was confirmed using standard bisulphite PCR.

Supplemental Figure S3.
Confirmation of allelic methylation at novel ubiquitously imprinted DMRs.
The methylation profiles obtained using leukocyte-, brain- and liver-derived WGBS, Infinium array datasets for the (A) *PPIEL*, (B) *WRB* and (C) *NHP2L1* genes. Vertical grey lines in the WGBS tracks represent the mean methylation value for individual CpG dinucleotides calculated from multiple data sets, with the light grey lines representing the mean + standard deviation. Infinium methylation values for normal tissues are represented by black dots, with values for the genome-wide UPDs (average pUPD in blue and mUPD in red) superimposed on the leukocyte methylation track. The methylation profiles were confirmed using standard allelic bisulphite PCR with each circle representing a single CpG dinucleotide on a DNA strand, (●, methylated cytosine; O unmethylated cytosine). Each row corresponds to an individual cloned sequence. The sequence analysis of RT-PCR products that differentiate *NHP2L1* variant transcripts reveals imprinting specifically of isoform-2 at this locus.

Supplemental Figure S4.
Specific hypermethylation of imprinted DMRs in placenta.
(A) The methylation profiles obtained using leukocyte- and placenta-derived WGBS, Infinium array datasets and allelic bisulphite PCR for *NNAT* DMR. Infinium methylation values for normal leukocytes (black dots), with values for the genome-wide pUPD (blue) and mUPD (red) superimposed on the leukocyte WGBS track. Similarly Infinium methylation values for normal placenta (black dots) and hydatidiform mole (blue dots) are overlaid on the placental WGBS track. The error bars associated with the Infinium array probes represent the standard deviation of multiple biological samples. The methylation profiles were confirmed using standard bisulphite PCR on heterozygous DNA samples with each circle representing a single CpG dinucleotide on a DNA strand, (●, methylated cytosine; O unmethylated cytosine). Each row corresponds to an individual cloned sequence. (B) The dynamic methylation profiles of the *NESP*-AS DMR as revealed by WGBS and Infinium array datasets in leukocytes, placenta, sperm, phES cells and hES cells, along with meDIP-seq and H3K4me3 ChIP-seq reads for hES cells and sperm. The grey and black dots in the third panel represent Infinium probe methylation in hES cell lines derived from six-cell blastomeres and blostocytes, respectively. The gametic WGBS methylation profile is derived from sperm, with Infinium probe methylation values for sperm and phES cells represented by blue and red dots. The error bars associated with the Infinium array probes represent the standard deviation of the 2 sperm samples and 4 independent phES cells cell lines. The methylation profiles were confirmed using standard bisulphite PCR and sequencing.

Downloaded from genome.cshlp.org on November 14, 2026 . Published by Cold Spring Harbor Laboratory Press

Supplemental Figure S5.
Confirmation of allelic methylation at placental-specific DMRs.
(A) The allelic methylation profiles in placenta for *ZFAT, N4BP2L1, DCAF10, PDE4D, FAM196A, RGMA, AGBL3, MCCC1, ZC3H12C, DNMT1, AIM1, ZNF396, FAM20A, GLIS3* and *LIN28B.* The methylation profiles were confirmed using standard allelic bisulphite PCR with each circle representing a single CpG dinucleotide on a DNA strand, (●, methylated cytosine; O unmethylated cytosine). Each row corresponds to an individual cloned sequence. (B) Allelic expression was performed on placental samples heterozygous for exonic SNPs. Where possible, parental genotypes were also determined. The asterisk (*) in the sequence traces shows the position of the polymorphic base.

Supplemental Figure S6.
Allelic methylation and expression analyses of murine loci orthologous human ubiquitous imprinted loci.
The allelic methylation analysis using embryonic genomic DNA from intersubspecific mouse crosses (C57BL6/J (B) with JF1 (J)) revealed the absence of parental origin-specific methylation in the *Nhp2l1, Wdr27, Wrb* and *Htr5a* loci. The methylation profiles were confirmed using standard allelic bisulphite PCR with each circle representing a single CpG dinucleotide on a DNA strand, (●, methylated cytosine; O unmethylated cytosine). Each row corresponds to an individual cloned sequence. These genes were found to be biallelically expressed in early embryonic tissues. The asterisk (*) in the sequence traces shows the position of the polymorphic base.

Supplemental Figure S7.
Allelic methylation and expression analyses of murine loci orthologous to human placental-specific imprinted loci.
(A) The allelic methylation using placental genomic DNA from intersubspecific mouse crosses (C57BL6/J (B) with JF1 (J) or *Mus musculus castaneous* (C)) reveals an unmethylated profile for all regions assessed. The methylation profiles were confirmed using standard allelic bisulphite PCR with each circle representing a single CpG dinucleotide on a DNA strand, (●, methylated cytosine; O unmethylated cytosine). Each row corresponds to an individual cloned sequence. (B) The sequences tracks of RT-PCR products incorporating heterozygous polymorphisms showing biallelic expression of transcripts in the placenta if detected. The asterisk (*) in the sequence traces shows the position of the polymorphic base.

Supplemental Figure S8.
Confirmation of differential methylation between parthenote-derived hES cells lines (phES) and sperm.
The orthologous sequences of germline imprinted DMRs in the mouse are highlighted by the hatched box with all Infinium probes mapping ± 1kb shown. phES cells are in red, sperm in blue. DMRs specific to mouse are marked with an asterisk (*) and are not differentially methylated.

Supplemental Figure S9.
Early developmental methylation dynamics at *NAPIL5* and *FAM50B* gene.

Downloaded from genome.cshlp.org on November 14, 2026 . Published by Cold Spring Harbor Laboratory Press

(A) Contraction of the *NAPIL5* germline DMRs. WGBS and Infinium array datasets in leukocytes, sperm, phES cells and hES cells, along with meDIP-seq and H3K4me3 ChIP-seq reads for hES cells and sperm. The grey and black dots in the second panel represent Infinium probe methylation in hES cell lines derived from six-cell blastomeres (Val10B) and blastocysts (SHEF5), respectively. The gametic WGBS methylation profile is derived from sperm, with Infinium probe methylation values for sperm and phES cells represented by blue and red dots respectively. The error bars associated with the Infinium array probes represent the standard deviation of the 2 sperm samples and 4 independent phES cells cell lines. The extended interval of differential methylation between sperm and phES cells was confirmed using standard bisulphite PCR. Each circle representing a single CpG dinucleotide on a DNA strand, (●, methylated cytosine; O unmethylated cytosine) and each row corresponds to an individual cloned sequence. (B) The relocation of the *FAM50B* DMR during pre-implantation development. The colour code for the Infiunium array datasets superimposed on the WGBS track is the same as in (A). The methylation profile was confirmed using three different bisulphite PCRs mapping within the interval.

Supplemental Figure S10.
The analysis of ZFP57 binding motifs in human imprinted DMRs.
The H3K9me3 distribution at (A) ubiquitous germline imprinted DMRs and (B) placenta-specific DMRs in the H1 hES cells in relation to DNA methylation. The % methylation is derived from WGBS data, where as the grey shaded area depicts H3K9me3 abundance determined from ChIP-seq data. The number and location of the proposed TGCC^{met}GC hexonucleotide ZFP57 binding motif are shown (Z). The precise location of the DMRs are shown by the red brackets.

References

Amor DJ, Halliday J. 2008. A review of known imprinting syndromes and their association with assisted reproduction technologies. *Hum Reprod* **23**: 2826-2834.

Baglivo I, Esposito S, De Cesare L, Sparago A, Anvar Z, Riso V, Cammisa M, Fattorusso R, Grimaldi G, Riccio A, et al. 2013. Genetic and epigenetic mutations affect the DNA binding capability of human ZFP57 in transient neonatal diabetes type 1. **FEBS Lett** *587*:1474-81.

Barbaux S, Gascoin-Lachambre G, Buffat C, Monnier P, Mondon F, Tonanny MB, Pinard A, Auer J, Bessières B, Barlier A, et al. 2012. A genome-wide approach reveals novel imprinted genes expressed in the human placenta. *Epigenetics* **7**: 1079-1090.

Bourc'his D, Xu GL, Lin CS, Bollman B, Bestor TH. 2001. Dnmt3L and the establishment of maternal genomic imprints. Science **294**: 2536-9.

Buiting K. 2010. Prader-Willi syndrome and Angelman syndrome. *Am J Med Genet C Semin Med Genet* **154C**: 365-376.

Choufani S, Shuman C, Weksberg R. 2010. Beckwith-Wiedemann syndrome. *Am J Med Genet C Semin Med Genet* **154C**: 343-354.

Constância M, Kelsey G, Reik W. 2004. Resourceful imprinting. *Nature* **432**: 53-

Downloaded from genome.cshlp.org on November 14, 2026 . Published by Cold Spring Harbor Laboratory Press

Ciccone DN, Su H, Hevi S, Gay F, Lei H, Bajko J, Xu G, Li E, Chen T. 2009. KDM1B is a histone H3K4 demethylase required to establish maternal genomic imprints. *Nature* **461**: 415-418.

Coombes C, Arnaud P, Gordon E, Dean W, Coar EA, Williamson CM, Feil R, Peters J, Kelsey G. 2003. Epigenetic properties and identification of an imprint mark in the Nesp-Gnasxl domain of the mouse Gnas imprinted locus. *Mol Cell Biol* **23**: 5475-5488.

Cooper WN, Constância M. 2010. How genome-wide approaches can be used to unravel the remaining secrets of the imprintome. *Brief Funct Genomics* **9**: 315-328.

Das R, Lee YK, Strogantsev R, Jin S, Lim YC, Ng PY, Lin XM, Chng K, Yeo GSh, Ferguson-Smith AC, Ding C. 2013. DNMT1 and AIM1 Imprinting in human placenta revealed through a genome-wide screen for allele-specific DNA methylation. *BMC Genomics* **14**: 685.

Dhayalan A, Rajavelu A, Rathert P, Tamas R, Jurkowska RZ, Ragozin S, Jeltsch A. 2010. The Dnmt3a PWWP domain reads histone 3 lysine 36 trimethylation and guides DNA methylation. *J Biol Chem* **285**: 26114-26120.

Eggermann T. 2010. Russell-Silver syndrome. *Am J Med Genet C Semin Med Genet* **154C**: 355-364.

Ehrlich M, Gama-Sosa MA, Huang LH, Midgett RM, Kuo KC, McCune RA, Gehrke C. 1982. Amount and distribution of 5-methylcytosine in human DNA from different types of tissues of cells. *Nucleic Acids Res* **10**: 2709-2721.

El-Maarri O, Buiting K, Peery EG, Kroisel PM, Balaban B, Wagner K, Urman B, Heyd J, Lich C, Brannan CI, et al. 2001. Maternal methylation imprints on human chromosome 15 are established during or after fertilization. *Nat Genet* **27**: 41-44.

Fedoriw AM, Stein P, Svoboda P, Schultz RM, Bartolomei M. 2004 Transgenic RNAi reveals essential function for CTCF in H19 gene imprinting. *Science* **303**: 238-240.

Fuke C, Shimabukuro M, Petronis A, Sugimoto J, Oda T, Miura K, Miyazaki T, Ogura C, Okazaki Y, Jinno Y. 2004. Age related changes in 5-methylcytosine content in human peripheral leukocytes and placentas: an HPLC-based study. *Ann Hum Genet* **68**:196-204.

Geuns E, De Temmerman N, Hilven P, Van Steirteghem A, Liebaers I, De Rycke M, et al. 2007. Methylation analysis of the intergenic differentially methylated region of DLK1-GTL2 in human. *Eur J Hum Genet* **15:** 352-631.

Downloaded from genome.cshlp.org on November 14, 2026 . Published by Cold Spring Harbor Laboratory Press

Gregg C, Zhang J, Weissbourd B, Luo S, Schroth GP, Haig D, Dulac C. 2010. High-resolution analysis of parent-of-origin allelic expression in the mouse brain. *Science* **329**: 643-648.

Hammoud SS, Nix DA, Zhang H, Purwar J, Carrell DT, Cairns BR. 2009. Distinctive chromatin in human sperm packages genes for embryo development. *Nature* **460**: 473-478.

Harness JV, Turovets NA, Seiler MJ, Nistor G, Altun G, Agapova LS, Ferguson D, Laurent LC, Loring JF, Keirstead HS. 2011. Equivalence of conventionally-derived and parthenote-derived human embryonic stem cells. *PLoS One* **6**: e14499.

Hata, K, Okano M, Lei H, Li E. 2002. Dnmt3L cooperates with the Dnmt3 family of de novo DNA methyltransferases to establish maternal imprints in mice. *Development* **129**: 1983-1993.

Hayashizaki Y, Shibata H, Hirotsune S, Sugino H, Okazaki Y, Sasaki N, Hirose K, Imoto H, Okuizumi H, Muramatsu M, et al. 1994. Identification of an imprinted U2af binding protein related sequence on mouse chromosome 11 using the RLGS method. *Nat Genet* **6**: 33-40.

Heyn H, Li N, Ferreira HJ, Moran S, Pisano DG, Gomez A, Diez J, Sanchez-Mut JV, Setien F, Carmona FJ, et al. 2012. Distinct DNA methylomes of newborns and centenarians. *Proc Natl Acad Sci USA* **109**: 10522-10527.

Hiura H, Sugawara A, Ogawa H, John RM, Miyauchi N, Miyanari Y, Horiike T, Li Y, Yaegashi N, Sasaki H, et al. 2010. A tripartite paternally methylated region within the Gpr1-Zdbf2 imprinted domain on mouse chromosome 1 identified by meDIP-on-chip. *Nucleic Acids Res* **38**: 4929-4945.

Iglesias-Platas, I, Court F, Camprubi C, Sparago A, Guillaumet-Adkins A, Martin-Trujillo A, Riccio A, Moore GE, Monk D. 2013. Imprinting at the PLAGL1 domain is contained within a 70-kb CTCF/cohesin-mediated non-allelic chromatin loop. *Nucleic Acids Res* **41**: 2171-2179.

Kagami M, O'Sullivan MJ, Green AJ, Watabe Y, Arisaka O, Masawa N, Matsuoka K, Fukami M, Matsubara K, Kato F, et al. 2010. The IG-DMR and the MEG3-DMR at human chromosome 14q32.2: hierarchical interaction and distinct functional properties as imprinting control centers. *PLoS Genet* **6**: e1000992.

Kagami M, Sekita Y, Nishimura G, Irie M, Kato F, Okada M, Yamamori S, Kishimoto H, Nakayama M, Tanaka Y, et al. 2008. Deletions and epimutations affecting the human 14q32.2 imprinted region in individuals with paternal and maternal upd(14)-like phenotypes. *Nat Genet* **40**: 237-242.

Kelsey G, Bodle D, Miller HJ, Beechey CV, Coombes C, Peters J, Williamson CM. 1999. Identification of imprinted loci by methylation-sensitive

Downloaded from genome.cshlp.org on November 14, 2026 . Published by Cold Spring Harbor Laboratory Press

representational difference analysis: application to mouse distal chromosome 2. *Genomics* **62**: 129-138.

Kelsey, G. 2010. Imprinting on chromosome 20: tissue-specific imprinting and imprinting mutations in the GNAS locus. *Am J Med Genet C Semin Med Genet* **154C**: 377-386.

Kobayashi H, Sakurai T, Imai M, Takahashi N, Fukuda A, Yayoi O, Sato S, Nakabayashi K, Hata K, Sotomaru Y, et al. 2012. Contribution of intragenic DNA methylation in mouse gametic DNA methylomes to establish oocyte-specific heritable marks. *PLoS Genet* **8**: e1002440.

Kobayashi H, Yanagisawa E, Sakashita A, Sugawara N, Kumakura S, Ogawa H, Akutsu H, Hata K, Nakabayashi K, Kono T. 2013. Epigenetic and transcriptional features of the novel human imprinted lncRNA GPR1AS suggest it is a functional ortholog to mouse Zdbf2linc. *Epigenetics* **8**: 635-645.

Kong A, Steinthorsdottir V, Masson G, Thorleifsson G, Sulem P, Besenbacher S, Jonasdottir A, Sigurdsson A, Kristinsson KT, Jonasdottir A, et al. 2009. Parental origin of sequence variants associated with complex diseases. *Nature* **462**: 868-874.

Lapunzina P, Monk D. 2011. The consequences of uniparental disomy and copy number neutral loss-of-heterozygosity during human development and cancer. *Biol Cell* **103**: 303-317.

Li X, Ito M, Zhou F, Youngson N, Zuo X, Leder P, Ferguson-Smith AC. 2008. A maternal-zygotic effect gene, Zfp57, maintains both maternal and paternal imprints. *Dev Cell* **15**: 547-557.

Lister R, Pelizzola M, Dowen RH, Hawkins RD, Hon G, Tonti-Filippini J, Nery JR, Lee L, Ye Z, Ngo QM, et al. 2009. Human DNA methylomes at base resolution show widespread epigenomic differences. *Nature* **462**: 315-3122.

Lopes S, Lewis A, Hajkova P, Dean W, Oswald J, Forné T, Murrell A, Constância M, Bartolomei M, Walter J, et al. 2003. Epigenetic modifications in an imprinting cluster are controlled by a hierarchy of DMRs suggesting long-range chromatin interactions. *Hum Mol Genet* **12**: 295-305.

Mackay DJ, Temple IK. (2010). Transient neonatal diabetes mellitus type 1. *Am J Med Genet C Semin Med Genet* **154C**: 335-342.

Mai Q, Yu Y, Li T, Wang L, Chen MJ, Huang SZ, Zhou C, Zhou Q. 2007. Derivation of human embryonic stem cell lines from parthenogenetic blastocysts. Cell Res 17: 1008-12.

Molaro A, Hodges E, Fang F, Song Q, McCombie WR, Hannon GJ, Smith AD. 2011. Sperm methylation profiles reveal features of epigenetic inheritance and evolution in primates. *Cell* **146**: 1029-1041.

Downloaded from genome.cshlp.org on November 14, 2026 . Published by Cold Spring Harbor Laboratory Press

Monk D, Arnaud P, Apostolidou S, Hills FA, Kelsey G, Stanier P, Feil R, Moore GE. 2006. Limited evolutionary conservation of imprinting in the human placenta. *Proc Natl Acad Sci USA* **103**: 6623-6628.

Monk D. 2010. Deciphering the cancer imprintome. *Brief Funct Genomics* **9**: 329-339.

Nakabayashi K, Trujillo AM, Tayama C, Camprubi C, Yoshida W, Lapunzina P, Sanchez A, Soejima H, Aburatani H, Nagae G, et al. 2011. Methylation screening of reciprocal genome-wide UPDs identifies novel human-specific imprinted genes. *Hum Mol Genet* **20**: 3188-3197.

Nakamura T, Arai Y, Umehara H, Masuhara M, Kimura T, Taniguchi H, Sekimoto T, Ikawa M, Yoneda Y, Okabe M. 2007. PGC7/Stella protects against DNA demethylation in early embryogenesis. *Nat Cell Biol* **9**: 64-71.

Noguer-Dance M, Abu-Amero S, Al-Khtib M, Lefèvre A, Coullin P, Moore GE, Cavaillé J. 2010. The primate-specific microRNA gene cluster (C19MC) is imprinted in the placenta. *Hum Mol Genet* **19**: 3566-3582.

Okae H, Hiura H, Nishida Y, Funayama R, Tanaka S, Chiba H, Yaegashi N, Nakayama K, Sasaki H, Arima T. 2011. Re-investigation and RNA sequencing-based identification of genes with placenta-specific imprinted expression. *Hum Mol Genet* **21**: 548-558.

Park KY, Sellars EA, Grinberg A, Huang SP, Pfeifer K. 2004. The H19 differentially methylated region marks the parental origin of a heterologous locus without gametic DNA methylation. *Mol Cell Biol* **24**: 3588-3595.

Proudhon C, Duffié R, Ajjan S, Cowley M, Iranzo J, Carbajosa G, Saadeh H, Holland ML, Oakey RJ, Rakyan VK, et al. 2012. Protection against de novo methylation is instrumental in maintaining parent-of-origin methylation inherited from the gametes. Mol *Cell* **47**: 909-920.

Quenneville S, Verde G, Corsinotti A, Kapopoulou A, Jakobsson J, Offner S, Baglivo I, Pedone PV, Grimaldi G, Riccio A, et al. 2011. In embryonic stem cells, ZFP57/KAP1 recognize a methylated hexanucleotide to affect chromatin and DNA methylation of imprinting control regions. *Mol Cell* **44**: 361-372.

Ramowitz LK, Bartolomei MS. 2011. Genomic imprinting: recognition and marking of imprinted loci. *Curr Opin Genet Dev* **22**: 72-78.

Romanelli V, Nevado J, Fraga M, Trujillo AM, Mori MÁ, Fernández L, Pérez de Nanclares G, Martínez-Glez V, Pita G, Meneses H, et al. 2011. Constitutional mosaic genome-wide uniparental disomy due to diploidisation: an unusual cancer-predisposing mechanism. *J Med Genet* **48**: 212-216.

Schroeder DI, Blair JD, Lott P, Yu HO, Hong D, Crary F, Ashwood P, Walker C, Korf I, Robinson WP, et al. 2013. The human placenta methylome. *Proc Natl Acad Sci USA* **110**: 6037-6042.

Downloaded from genome.cshlp.org on November 14, 2026 . Published by Cold Spring Harbor Laboratory Press

Sharp A, Migliavacca E, Dupre Y, Stathaki E, Reza Sailani M, Baumer A, Schinzel A, Mackay DJ, Robinson DO, Cobellis G, et al. 2010. Methylation profiling in individuals with uniparental disomy identify novel differentially methylated regiosn on chromosome 15. *Genome Res* **20**: 1271-1278.

Smallwood SA, Tomizawa S, Krueger F, Ruf N, Carli N, Segonds-Pichon A, Sato S, Hata K, Andrews SR, Kelsey G. 2011. Dynamic CpG island methylation landscape in oocytes and pre-implantation embryos. *Nat Genet* **43**: 811-814.

Smith ZD, Chan MM, Mikkelsen TS, Gu H, Gnirke A, Regev A, Meissner A. 2012. A unique regulatory phase of DNA methylation in the early mammalian embryo. *Nature* **484**: 339-344.

Thomson JP, Skene PJ, Selfridge J, Clouaire T, Guy J, Webb S, Kerr AR, Deaton A, Andrews R, James KD, et al. 2010. CpG islands influence chromatin structure via the CpG-binding protein Cfp1. *Natur*e **464**: 1082-1086.

Tomizawa S, Kobayashi H, Watanabe T, Andrews S, Hata K, Kelsey G, Sasaki H., 2011. Dynamic stage-specific changes in imprinted differentially methylated regions during early mammalian development and prevalence of non-CpG methylation in oocytes. *Development* **138**: 811-820.

Umlauf D, Goto Y, Cao R, Cerqueira F, Wagschal A, Zhang Y, Feil R. 2004. Imprinting along the Kcnq1 domain on mouse chromosome 7 involves repressive histone methylation and recruitment of Polycomb group complexes. *Nat Genet* **36**: 1296-1300.

Wood AJ, Schulz R, Woodfine K, Koltowska K, Beechey CV, Peters J, Bourc'his D, Oakey RJ. 2008. Regulation of alternative polyadenylation by genomic imprinting. *Genes Dev* **22**: 1141-1146.

Xie W, Barr CL, Kim A, Yue F, Lee AY, Eubanks J, Dempster EL, Ren B. 2012. Base-resolution analyses of sequence and parent-of-origin dependent DNA methylation in the mouse genome. *Cell* **148**: 816-831.

Yamazawa K, Nakabayashi K, Kagami M, Sato T, Saitoh S, Horikawa R, Hizuka N, Ogata T. 2010. Parthenogenetic chimaerism/mosaicism with a Silver-Russell syndrome-like phenotype. *J Med Genet* **47**, 782-785.

Yuen RKC, Jiang R, Penaherrera M, McFadeen DE, Robinson WP. 2011. Genome-wide mapping of imprinted differentially methylated regions by DNA methylation profiling of human placentas from triploidies. *Epigenetics & Chromatin* **4**:10.

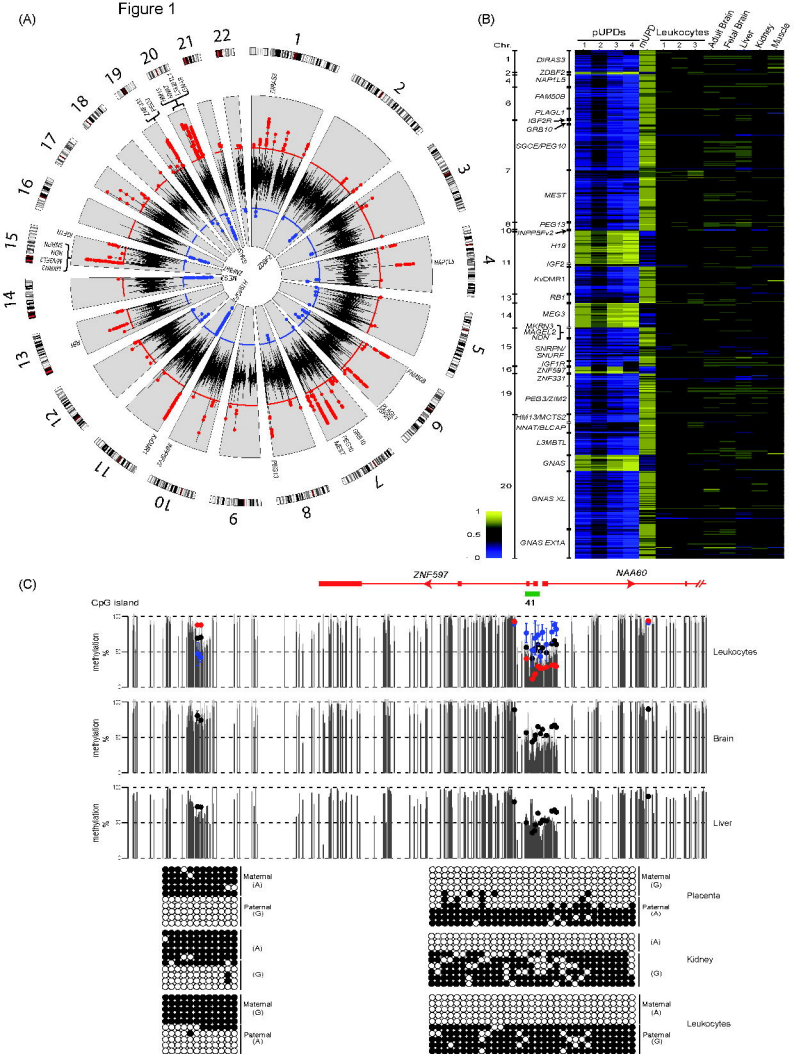
Zeng J, Konopka G, Hunt BG, Preuss TM, Geschwind D, Yi SV. 2012. Divergent whole-genome methylation maps of human and chimpanzee brains reveal epigenetic basis of human regulatory evolution. Am *J Hum Genet* **91**: 455-465.

Downloaded from genome.cshlp.org on November 14, 2026 . Published by Cold Spring Harbor Laboratory Press

Zhang Y, Jurkowska R, Soeroes S, Rajavelu A, Dhayalan A, Bock I, Rathert P, Brandt O, Reinhardt R, Fischle W, et al. 2010. Chromatin methylation activity of Dnmt3a and Dnmt3a/3L is guided by interaction of the ADD domain with the histone H3 tail. *Nucleic Acids Res* **38**: 4246-42.

Downloaded from genome.cshlp.org on November 14, 2026 . Published by Cold Spring Harbor Laboratory Press

Figure 1


(A)
(B)
(C)
pUPDs
Leukocytes
Adult Brain
Fetal Brain
Liver
Kidney
Muscle
Chr
DIRAS3
ZDBF2
NAPIL5
FAM50B
FLJ43967
IGF2R
GRB10
SGCE/PEG10
MEST
PEG13
PPP1R9A
H19
IGF2
KvDMR1
RB1
MEG3
MKRN3
MAGEL2
NDN
SNURF/
SNURF
IGF1R
ZNF597
ZNF331
PEG3/ZIM2
TSSC5
TSPAN32
NNAT/BLCAP
L3MBTL
GNAS
GNAS XL
GNAS EXTA
ZNF597
NAA60
CpG island
methylation %
Leukocytes
Brain
Liver
Maternal
(A)
Paternal
(G)
Placenta
Kidney
Leukocytes

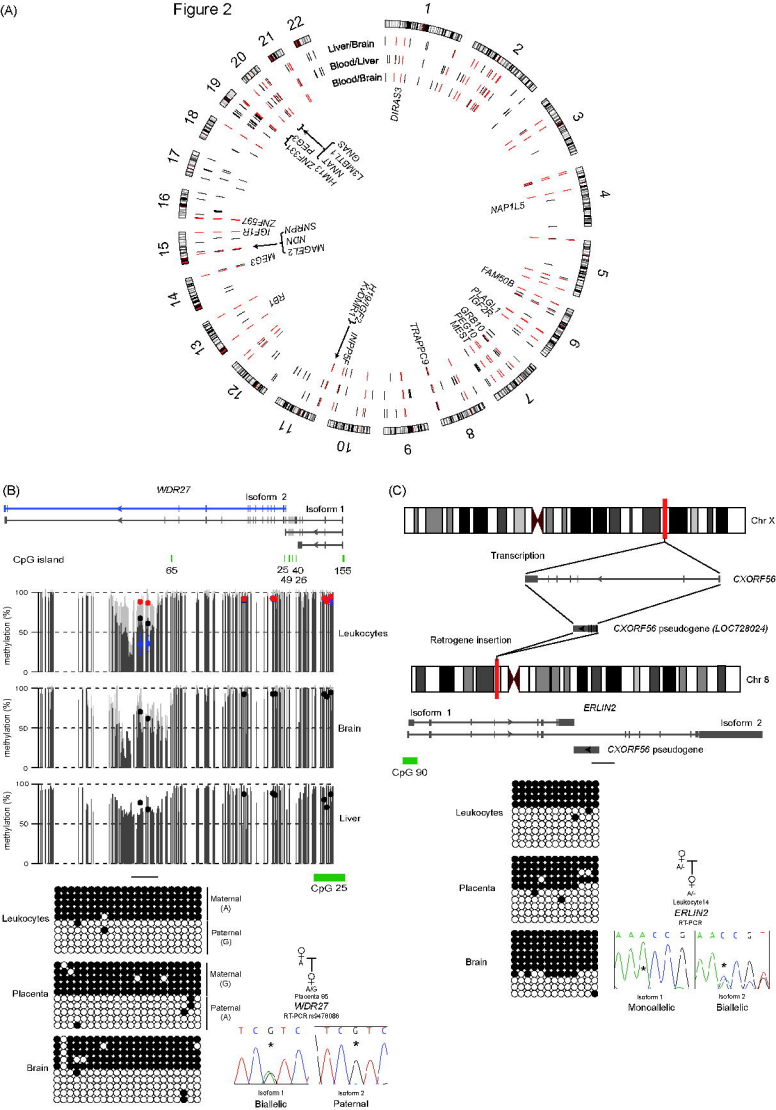
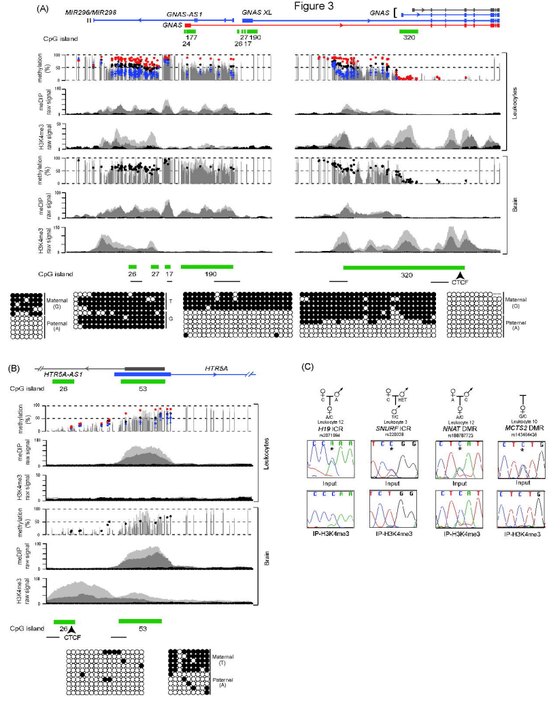

Figure 2
(A)
Liver/Brain
Blood/Liver
Blood/Brain
DIRAS3
MAP1L5
FAM60B
PLAGL1
HTR5A
GRB10
PEG10
MEST
TRAPPC9
NR5A2
KCNMB1
RBM26
RBI
MAGEL2
NDN
SNRPN
IGF1R
ZNF597
ME03
HM13
ZNF331
L3MBTL1
NKAT1
PSG9
GNAS
(B)
WDR27
Isoform 2
Isoform 1
CpG island
65
25 40
49 26
155
Leukocytes
Brain
Liver
methylation (%)
100
50
0
CpG 25
Maternal (A)
Paternal (G)
Maternal (G)
Paternal (A)
Placenta 66
WDR27
RT-PCR rs478086
Isoform 1
Isoform 2
Biallelic
Paternal
(C)
Chr X
Transcription
CXORF56
Retrogene insertion
CXORF56 pseudogene (LOC728024)
Chr 8
ERLIN2
Isoform 1
Isoform 2
CXORF56 pseudogene
CpG 90
Leukocyte14
ERLIN2
RT-PCR
Monoallelic
Biallelic

Figure 3


(A)
MIR296/MIR298
GNAS-AS1
GNAS XL
GNAS
GNAS
CpG island
177
24
27
26
17
190
320
methylation (%)
meDIP raw signal
H3K4me3 raw signal
Leukocytes
Brain
CpG island
26
27
17
190
320
CTCF
Maternal (G)
Paternal (A)
(B)
HTR5A-AS1
HTR5A
CpG island
26
53
Leukocytes
Brain
CTCF
Maternal (T)
Paternal (A)
(C)
Leukocyte 12
H19 ICR
rs2071094
Leukocyte 3
SNURF-ICR
rs220939
Leukocyte 12
NNAT DMR
rs16897725
Leukocyte 16
MCTS2 DMR
rs14340424
Input
IP-H3K4me3

Downloaded from genome.cshlp.org on November 14, 2026 . Published by Cold Spring Harbor Laboratory Press

Figure 4

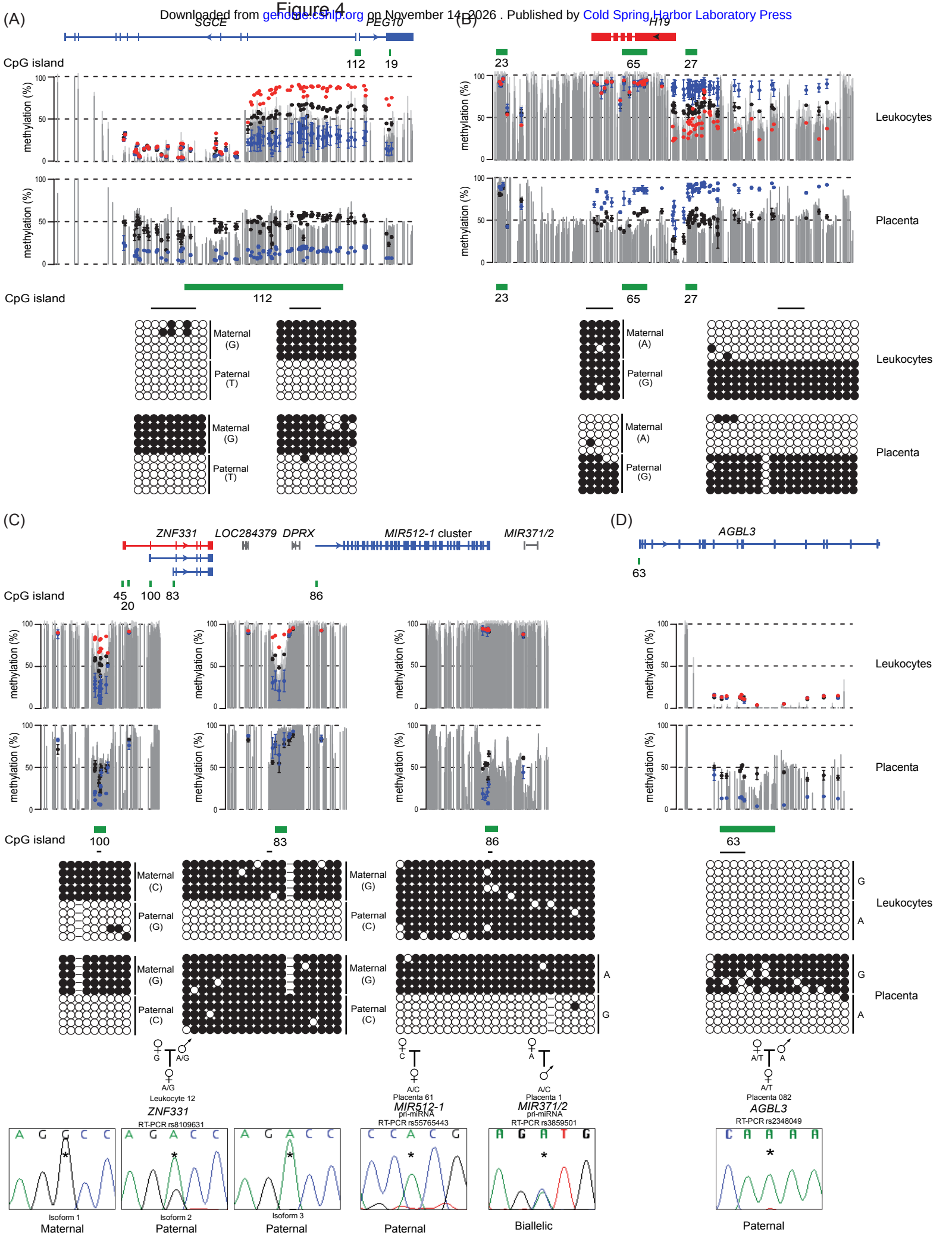
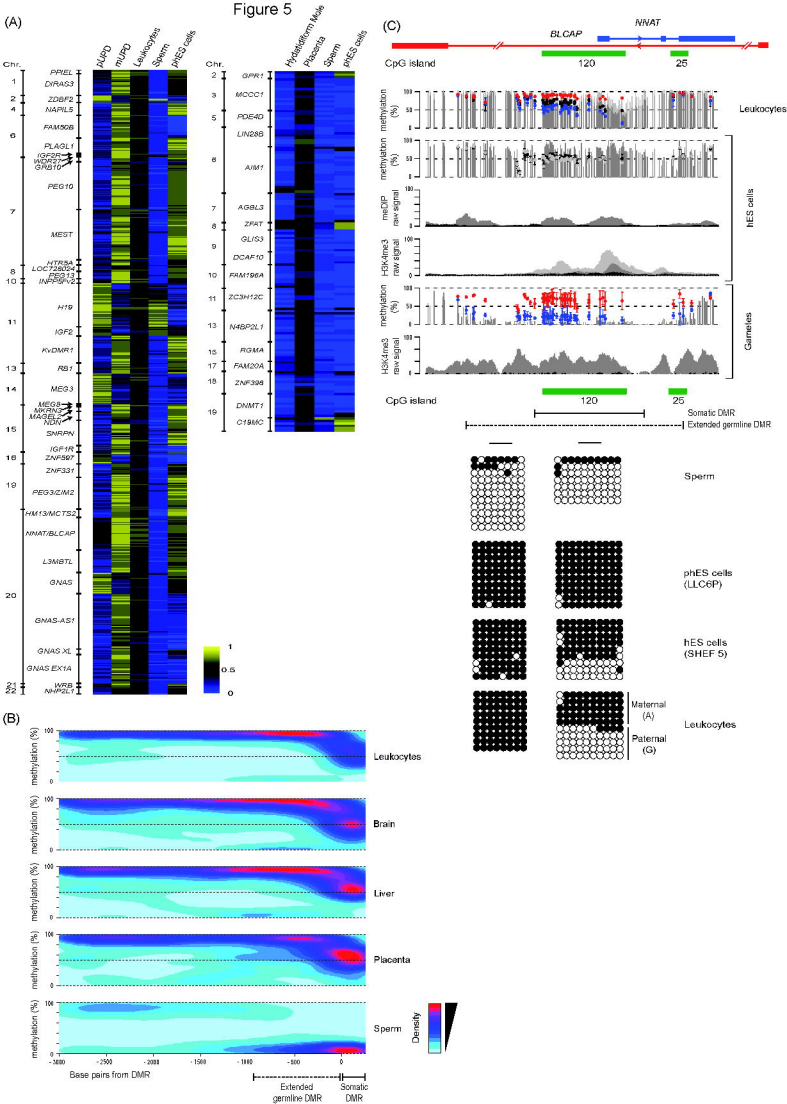


Figure 5


(A)
pUPD
muPD
Leukocytes
Sperm
phES cells
Chr.
PREL
DIRAS3
ZDBF2
NAPIL5
PEG10
MEST
HTR5A
LOC728024
PEG13
INPP5Q-AS2
H19
IGF2
KvDMR1
RB1
MEG3
MEG8
MKRN3
MAGEL2
NDN
SNRPN
IGF1R
ZNF597
ZNF331
PEG3/ZIM2
NHP13/MCTS2
NNAT/BLCAP
L3MBTL
GNAS
GNAS-AS1
GNAS XL
GNAS EX1A
WRB
NHP2L1
Hydatidiform Mole
Placenta
Sperm
phES cells
GPR1
MCCC1
PDE4D
LIN28B
AIM1
AGBL3
ZFAT
GLIS3
DCAF10
FAM196A
ZC3H12C
N4BP2L1
RGMA
FAM20A
ZNF396
DNMT1
C19MC
1
0.5
0
(C)
BLCAP
NNAT
CpG island
120
25
methylation (%)
Leukocytes
meDIP raw signal
H3k4me3 raw signal
hES cells
Gametes
Somatic DMR
Extended germline DMR
Sperm
phES cells (LLC6P)
hES cells (SHEF 5)
Maternal (A)
Paternal (G)
Leukocytes
(B)
Leukocytes
Brain
Liver
Placenta
Sperm
Density
Base pairs from DMR
Extended germline DMR
Somatic DMR

Known Imprinted DMRs (n=36)								Novel DMRs (n=25) Novel DMRs near known Imprinted Loci (n=8)							
Gene Locus	Chr	Extent (WGBS) Start	Extent (WGBS) Finish	# Infinium probes	GC Content	# CpG	Methylation origin	Gene Locus	Chr	Extent (WGBS) Start	Extent (WGBS) Finish	# Infinium probes	GC Content	# CpG	Methylation origin
DIRAS3	1	68515433	68517545	17	0.50	88	M	*DIRAS3* Ex2	1	68512505	68513486	8	0.52	39	M
ZDBF2	2	207114583	207136544	8	0.45	439	P	*MEG8*	14	101370741	101371419	1	0.66	43	M
NAP1L5	4	89618184	89619237	15	0.57	57	M	*SNRPN* intragenic CpG32	15	24346736	24347142	1	0.59	30	M
FAM50B	6	3849082	3850359	25	0.65	90	M	*SNRPN* intragenic CpG29	15	24671872	24672679	4	0.59	39	M
PLAGL1	6	144328078	144329888	16	0.58	143	M	*SNRPN* intragenic CpG30	15	24722753	24723071	1	0.66	29	M
IGF2R	6	160426558	160427561	2	0.70	74	M	*SNRPN* intragenic CpG40	15	25017924	25018886	4	0.51	67	M
GRB10	7	50848726	50851312	9	0.60	171	M	*ZNF597*	16	3481801	3482388	2	0.54	29	M
PEG10	7	94285537	94287960	53	0.60	119	M	*ZNF331*	19	54057086	54058425	4	0.66	102	M
MEST	7	130130122	130134388	55	0.54	226	M								
TRAPPC9	8	141108147	141111081	8	0.62	193	M	Novel DMRs (n=6)							
INPP5F	10	121578046	121578727	4	0.59	52	M	*PPIEL*	1	40024626	40025540	4	0.54	39	M
H19	11	2018812	2024740	48	0.60	250	P	*WDR27*	6	170054504	170055618	2	0.56	58	M
IGF2 DMR2	11	2153991	2155112	9	0.65	63	P	*HTR5A*	7	154862719	154863382	6	0.62	55	M
IGF2 DMR0	11	2168333	2169768	1	0.62	33	P	*CXORF56 pseudogene/ERLIN2*	8	37604992	37606088	7	0.45	37	M
KvDMR1	11	2719948	2722259	30	0.67	192	M	*WRB*	21	40757510	40758276	4	0.61	43	M
RB1	13	48892341	48895763	12	0.59	195	M	*NHP2L1*	22	42077774	42078873	8	0.54	63	M
IG-DMR	14	101275427	101278058	0	0.52	64	P								
MEG3	14	101290524	101293978	33	0.60	188	P	Known Imprinted DMRs (n=2) & novel DMRs (n=15)							
MKRN3/ MIR4508	15	23807086	23812495	12	0.44	109	M	Placental-specific DMRs (n=17)							
MAGEL2	15	23892425	23894029	6	0.55	51	M	*GPR1-AS*	2	207066967	207069445	3	0.49	86	M
NDN	15	23931451	23932759	8	0.65	108	M	*MCCC1*	3	182815725	182817627	13	0.54	94	M
SNRPN	15	25068564	25069481	8	0.42	19	M	*PDE4D*	5	58333774	58336554	7	0.54	145	M
SNRPN	15	25093008	25093829	4	0.49	44	M	*LIN28B*	6	105400631	105402559	8	0.45	62	M
SNRPN	15	25123027	25123905	5	0.47	45	M	*AIM1*	6	106957945	106961974	19	0.54	203	M
SNURF	15	25200004	25201976	7	0.60	113	M	*AGBL3*	7	134671024	134672011	12	0.59	74	M
IGF1R	15	99408496	99409650	7	0.51	55	M	*ZFAT*	8	135707227	135710114	3	0.60	111	M
ZNF597/NAA60	16	3492828	3494463	11	0.54	76	P	*GLIS3*	9	4297279	4300182	9	0.63	235	M
ZNF331	19	54040510	54042212	11	0.64	125	M	*DCAF10*	9	37800140	37802937	5	0.56	157	M
PEG3	19	57348493	57353271	36	0.59	221	M	*FAM196A/DOCK1*	10	128993405	128995242	10	0.72	198	M
MCTS2/HM13	20	30134663	30135933	9	0.48	47	M	*ZC3H12C*	11	109962727	109964784	9	0.66	198	M
BLCAP/NNAT	20	36148604	36150528	35	0.55	135	M	*N4BP2L1*	13	33000694	33002448	13	0.66	136	M
L3MBTL	20	42142365	42144040	25	0.65	84	M	*RGMA*	15	93614998	93616859	8	0.61	134	M
GNAS	20	57414039	57418612	23	0.57	257	P	*FAM20A*	17	66596155	66597643	4	0.72	162	M
NESP-AS/GNAS-AS1	20	57425649	57428033	62	0.61	128	M	*ZNF396*	18	32956510	32957580	9	0.64	86	M
GNAS XL	20	57428905	57431463	6	0.65	200	M	*MIR512-1* cluster	19	54150515	54155608	6	0.53	216	M
GNAS Ex1A	20	57463265	57465201	38	0.67	198	M	*DNMT1*	19	10303506	10306415	10	0.55	129	M

Downloaded from genome.cshlp.org on November 14, 2026 . Published by Cold Spring Harbor Laboratory Press